END

FILMED

DTIC

MICROCOPY RESOLUTION TEST CHART
NATIONAL BUREAU OF STANDARDS-1963-A

AD A121611

Atmospheric Effects in Low Earth Orbit and the DMSP ESA Offset Anomaly

G. S. ARNOLD, R. R. HERM, and D. R. PEPLINSKI
Chemistry and Physics Laboratory
Laboratory Operations
The Aerospace Corporation ·
El Segundo, Calif. 90245

30 September 1982

DTIC
ELECTE
NOV 1 9 1982

A

DTIC FILE COPY

82 11 19 010

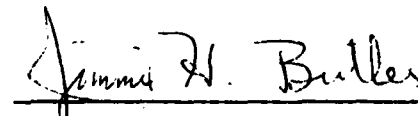This report was submitted by The Aerospace Corporation, El Segundo, CA 90245, under Contract No. F04701-81-C-0082 with the Space Division, Deputy for Technology, P.O. Box 92960, Worldway Postal Center, Los Angeles, CA 90009. It was reviewed and approved for The Aerospace Corporation by S. Feuerstein, Director, Chemistry and Physics Laboratory. Lt G. A. Welz, SD/YLVS, was the project officer for Technology.
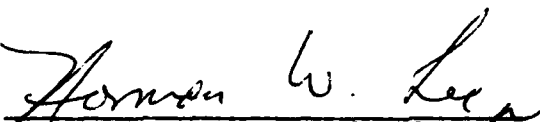
This report has been reviewed by the Public Affairs Office (PAS) and is releasable to the National Technical Information Service (NTIS). At NTIS, it will be available to the general public, including foreign nations.

This technical report has been reviewed and is approved for publication. Publication of this report does not constitute Air Force approval of the report's findings or conclusions. It is published only for the exchange and stimulation of ideas.

Gregory A. Welz, 2nd Lt, USAF
Project Officer

Jimmie H. Butler, Colonel, USAF
Director of Space Systems Planning

FOR THE COMMANDER

Norman W. Lee, Jr., Colonel, USAF
Deputy for Technology

REPORT DOCUMENTATION PAGE

READ INSTRUCTIONS
BEFORE COMPLETING FORM

1. REPORT NUMBER	2. GOVT ACCESSION NO.	3. RECIPIENT'S CATALOG NUMBER
SD-TR-82-81	AD-A121 611	

4. TITLE *(and Subtitle)*	5. TYPE OF REPORT & PERIOD COVERED
ATMOSPHERIC EFFECTS IN LOW EARTH ORBIT AND THE DMSP ESA OFFSET ANOMALY	
	6. PERFORMING ORG. REPORT NUMBER
	TR-0082(2478-20)-1

7. AUTHOR(s)	8. CONTRACT OR GRANT NUMBER(s)
Graham S. Arnold, Ronald R. Herm, and Daniel R. Peplinski	F04701-81-C-0082

9. PERFORMING ORGANIZATION NAME AND ADDRESS	10. PROGRAM ELEMENT, PROJECT, TASK AREA & WORK UNIT NUMBERS
The Aerospace Corporation El Segundo, Calif. 90245	

11. CONTROLLING OFFICE NAME AND ADDRESS	12. REPORT DATE
Space Division Air Force Systems Command Los Angeles, Calif. 90009	30 September 1982
	13. NUMBER OF PAGES
	58

14. MONITORING AGENCY NAME & ADDRESS*(if different from Controlling Office)*	15. SECURITY CLASS. *(of this report)*
	Unclassified
	15a. DECLASSIFICATION/DOWNGRADING SCHEDULE

16. DISTRIBUTION STATEMENT *(of this Report)*

Approved for public release; distribution unlimited

17. DISTRIBUTION STATEMENT *(of the abstract entered in Block 20, if different from Report)*

18. SUPPLEMENTARY NOTES

19. KEY WORDS *(Continue on reverse side if necessary and identify by ...er)*

Atmospheric Effects	DMSP
Atomic Beams	Germanium
Beam-Surface Chemistry	Oxygen Atoms
Contamination	RTV-615

20. ABSTRACT *(Continue on reverse side if necessary and identify by block number)*

A space vehicle in Earth orbit experiences bombardment with fast (about 8 km/sec) atmospheric particles, the principal of which is atomic oxygen, by virtue of its orbital velocity. Several satellite systems that have been or may be adversely affected by atmospheric impact are described. The current knowledge of the gas-surface interactions of atomic oxygen and the available experimental technology for laboratory simulation of atmospheric bombardment in orbit are reviewed. The DMSP ESA offset anomaly is described and evidence

DD FORM 1473
(FACSIMILE)

19. KEY WORDS (Continued)

20. ABSTRACT (Continued)

for linking this misbehavior to atmospheric oxygen atom impact is presented and discussed. The results of a laboratory experiment to test this link are presented.

ACKNOWLEDGMENTS

1

CONTENTS

FIGURES

TABLES

I. INTRODUCTION

As the period for which satellite missions are required to function increases, so the importance of the long-term effects of exposure of spacecraft materials to the upper atmosphere increases. The advent of the shuttle orbiter, operating at relatively low altitudes, places further importance upon the action of atmospheric species because of the higher atmospheric density encountered in low Earth orbit. The interactions of atmospheric species, the principal of which at orbital altitudes is atomic oxygen, with spacecraft materials are poorly understood. This results, to no small degree, from shortcomings in the experimental technology for simulating the orbital environment in the laboratory.

A brief description of the atmospheric effects that are encountered by a spacecraft in Earth orbit is provided in Section II. Some examples of satellite systems, which have been or may be affected by atmospheric impact, are presented. The present knowledge of the gas-surface interactions of atomic oxygen and the state-of-the-art in experimental technology for simulating atmospheric bombardment by oxygen atoms are reviewed.

The Defense Meteorological Satellite Program (DMSP) Earth Sensor Assembly (ESA) offset anomaly is described in Section III. Evidence for linking this misbehavior to atmospheric oxygen atom impact is presented. An experiment to test this link is outlined. The experimental apparatus is described in detail in Section IV, and in Section V the results of the experimental program are presented and discussed.

II. BACKGROUND

In this section a brief review of the atmospheric composition in low Earth orbit is presented. Several satellite systems, which have been or may be affected by atmospheric bombardment, are described. A review of the effects of oxygen atom interactions with surfaces is presented, and the state-of-the-art for production of atomic oxygen beams in the laboratory is described.

A. ATMOSPHERIC COMPOSITION

The composition and density of the atmosphere above 120 km are functions of several variables, such as local time, day of the year, geographic latitude, sunspot activity, radio solar flux, and magnetic index. Neutral species present at these altitudes include O, N_2, He, O_2, Ar, and H. Molecular nitrogen is the dominant atmospheric neutral specie below 200 km, whereas atomic oxygen dominates above 250 km. As one would expect, number densities of neutral species decrease with increasing altitude. For example, at sunspot maximum, the number density of oxygen atoms at 370 km is about 10^9 cm^{-3}, while at 830 km it is about 10^7 cm^{-3}. In Table 1 are shown the densities of the predominant atmospheric species at several altitudes. The dramatic variation of oxygen atom concentration with solar activity is shown in Fig. 1. The number densities of the neutral elements and molecules in the atmosphere have been modeled by Hedin.[1-3]

Ions are also present above 60 km.[4] The major ionic specie in the D region (60 to 85 km) is NO^+. In the E region (85 to 140 km), the most abundant ions are NO^+ and O_2^+. The NO^+ ion is formed by reaction of O^+, produced by solar x-rays, with N_2. Nitrogen molecules are also photoionized, but rapid dissociative recombination keeps the steady-state concentration of N_2^+ low. The F_1 region lies between 140 and approximately 200 km. The predominant ions at its lower boundary are NO^+ and O_2^+, whereas O^+ is the principal ion near its upper boundary. The principal ion of the F_2 region (200 to 1300 km) is O^+, with N^+ also present to a much lesser extent. At 830 km, the O^+ ion is approximately an order of magnitude lower in concentration

11

Table 1. Atmospheric Composition (cm^{-3})

Species[a]	Altitude (km)		
	200[b]	300[c]	800[d]
N_2	2.62×10^9	1.06×10^8	1.01×10^2
O_2	2.97×10^8	7.66×10^6	1.01
O	3.18×10^9	4.72×10^8	1.70×10^5
Ar	3.14×10^6	3.31×10^4	8.39×10^{-5}
He	5.16×10^6	3.11×10^6	4.28×10^5
H	1.92×10^5	1.63×10^5	9.88×10^4
NO+	3×10^5	1.5×10^4	-----
O_2+	8×10^4	6×10^3	-----
O+	8×10^4	5×10^5	5×10^4

[a]Ion concentrations from Ref. 64
[b]Temperature = 923 K
[c]Temperature = 1004 K
[d]Temperature = 1012 K

12
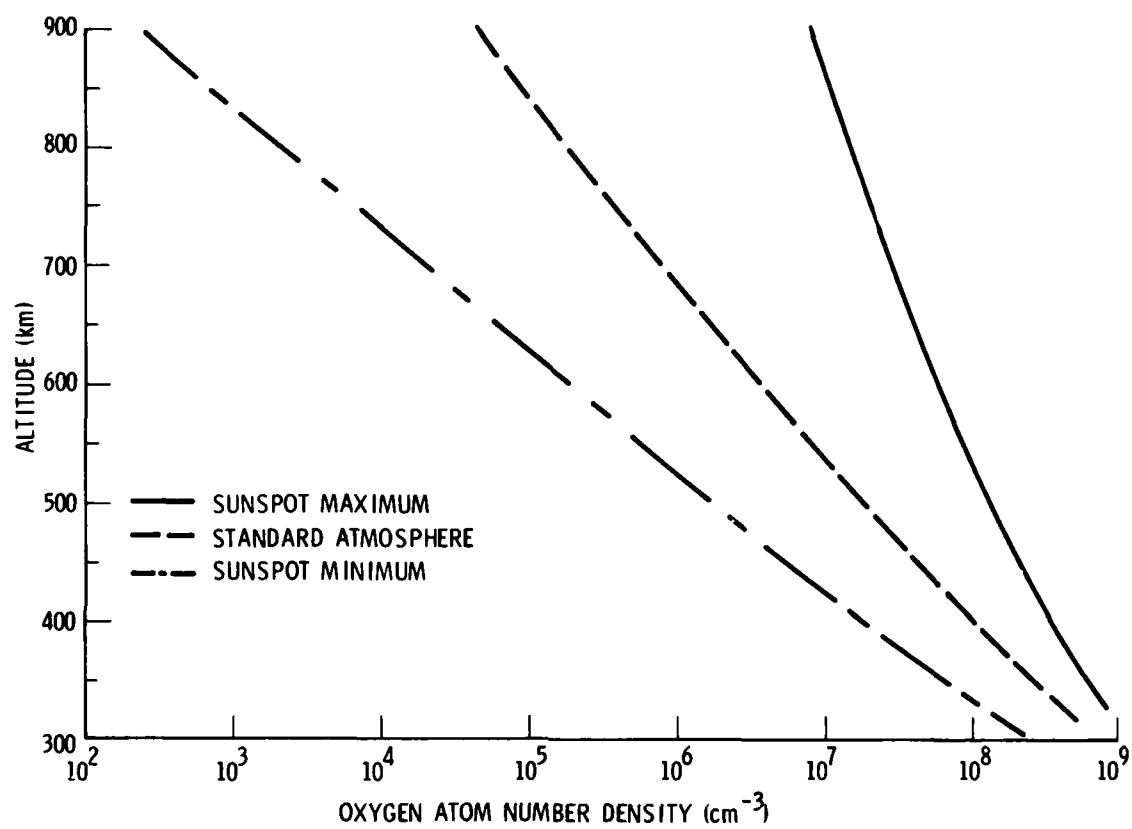
Fig. 1.   Oxygen Atom Number Density Profiles

13

than oxygen atoms. Velocities of O^+ ions are about 1 km sec^{-1}. Above 1300 km, protons dominate. The ionosphere is electrically neutral, in the sense that the positive ion density is equal to the electron and negative ion density at all heights.

A spacecraft in low Earth orbit is bombarded by the atmosphere. A vessel in orbit at 370 km, e.g., a shuttle sortie, with an assumed velocity of 8 km sec^{-1} is subjected to an oxygen atom flux of about 10^{14} cm^{-2} sec^{-1}. If all these atoms were condensed upon the surface, a monolayer would form every 10 sec. At 830 km, e.g., DMSP, the flux is about 10^{11} cm^{-2} sec^{-1}, or a monolayer in about 4 hr. Although the ambient atmospheric temperature is not high, about 1000 K, the orbital velocity causes the atmospheric particles to strike the spacecraft at high energies. The kinetic energies of 8 km sec^{-1} N_2, O, and He particles are approximately 9.3, 5.3, and 1.3 eV, respectively.

B. ATMOSPHERIC EFFECTS ON ORBIT

The atmosphere bombarding a spacecraft may interact with the surfaces of the vessel in a number of ways which affect the surface properties. Among these effects are: condensation, luminescence, sputtering, volatilization of weakly bound surface deposits, and chemical reactions with the surface or with impurities deposited thereon. Several satellite systems on which these effects have been observed, predicted to be a problem, or postulated are described herein.

1. ATMOSPHERE EXPLORER

Airglow measurements reported in 1977 performed by the Atmosphere Explorer C (AE-C) spacecraft have suffered interference produced by an as yet unexplained interaction with the neutral atmosphere at low altitudes.[5] This interference appears as an increase in the measured brightness that is approximately proportional to atmospheric density. The increase is greatest when the instrument is looking in the direction of motion of the satellite, but the effect is present at altitudes below 170 km even when the instrument is looking upward. The individual wavelengths, which the AE-C experiments monitored (as well as their origins), are listed in Table 2. Interference was present at all wavelengths monitored. The intensity of the interference increases at

14

Table 2. Atmosphere Explorer C Monitored Wavelengths

$\lambda(\text{Å})$	Transition
3371	$M_2(C^3\pi_u \rightarrow B^3\pi_g)$
4278	$N_2^+(B^2\Sigma_g^+ \rightarrow X^2\Sigma_u^+)$
5200	$N(^2D \rightarrow {}^4S)$
5577	$O(^1S \rightarrow {}^1D)$
6300	$O(^1D \rightarrow {}^3P)$
7319	$O^+(^2P \rightarrow {}^2D)$

15

longer wavelengths. The effect is so severe that otherwise successful observations coincident between AE-C and ground observatories had to be discarded when AE measurements were made below 170 km.[6] (AE-C was then in elliptical orbit.)

Subsequent measurements made during periods of increased solar activity show this effect to be present at altitudes as great as 400 km. Night-time measurements of 7319 Å emission confirm that the background is strongly dependent on the direction of the sensor, emission being strongest when the detector faces the atmospheric ram.[6]

When this effect was initially observed, it was hypothesized that the emission arose from the NO_2 continuum produced by reaction of atmospheric nitric oxide with oxygen atoms adsorbed on the spacecraft. This supposition has subsequently been proven incorrect.[6] Efforts are currently in progress at Harvard and the University of Michigan to provide a satisfactory explanation of this phenomenon.

2. DISCOVERERS 26 AND 32

Since particles in the orbital atmosphere impact upon spacecraft surfaces at high velocity, it is possible that surface material may be sputtered. Over a period of time, a surface of the space vehicle can be slowly eroded, result-ing in changes in various surface properties such as reflectivity or drag coefficient.

Direct measurements of surface erosion have been made by McKeown and co-workers[7-9] using quartz crystal microbalances[10] orbiting on the Air Force satellites Discoverers 26 and 32. Discoverer 26 was launched on 27 July 1961 into an elliptical orbit with apogee at 810 km and perigee at 228 km. Discoverer 32 was launched on 13 October 1961 into a 404 by 232 km elliptical orbit. The flights pass under the regions where protons and heavy ions arising from radiation belts, solar flares, and the solar corona are present. Thus any erosion of surfaces results from sputtering by molecules of the upper atmosphere or by micrometeoroid impact.

Gold surfaces normal to the velocity vector of the satellite, facing the atmospheric ram, were observed to erode at a rate of 0.2 to 0.3 Å/day. McKeown has interpreted this erosion as sputtering by impact with atmospheric nitrogen. Nitrogen molecules strike the Discoverer spacecraft with a collision energy of 9 eV. Sputtering rates were calculated to range from 10^{10} atoms cm^{-2} sec^{-1} at 200 km to 10^7 atoms cm^{-2} sec^{-1} at 800 km. These rates correspond to a sputtering probability of 5×10^{-6} Au/N_2.[7-9]

3. OGO-6

OGO-6 was launched on 5 June 1969 into a polar orbit with a perigee of 397 km and an apogee of 1098 km. Included on OGO-6 was an experiment to determine the rate of deposition of satellite outgassing material upon clean surfaces of the craft, as well as the rates at which the contaminated surfaces were cleaned by desorption and sputtering.[11]

The satellite outgassing flux consists of both volatile gases, such as O_2, N_2, CO_2, and H_2O, as well as higher molecular weight contaminants, such as outgassing, from adhesives and paints. The rates of spontaneous desorption and atmospheric sputtering of contaminants were measured by observing mass loss from contaminated surfaces after outgassing flux had dropped to a negligible level. The mass loss caused by desorption, measured with the experimental surfaces shielded from the atmospheric flux, was 1.2×10^{-9} $g\text{-}m^{-2}$ sec^{-1}.

The mass loss rate for the combined processes of sputtering and desorption was measured at two values of angle of incidence of the atmosphere. At normal incidence, the total mass loss was 3.5×10^{-9} $g\text{-}m^{-2}$ sec^{-1}, which implies a sputtering rate of 2.3×10^{-9} $g\text{-}m^{-2}$ sec^{-1}. At incidence of 76° from normal, these rates were 3.8×10^{-9} and 2.6×10^{-9} $g\text{-}m^{-2}$ sec^{-1}.

These sputtering rates are not for the gold or aluminum surfaces themselves, but rather they are for the contaminants deposited thereon. Assuming the contamination has an average molecular weight of 200, the probabilities of an atmospheric molecule sputtering a contaminant molecule upon impact ($P_{\theta i}$) are:[11]

$$P_0^° = 7 \times 10^{-5}$$

$$P_{76}^° = 3 \times 10^{-4}$$

The probability of sputtering is greater near grazing incidence because the impacting molecule may sputter a contaminant molecule without having to reverse the direction of its momentum.

4. SATELLITE INFRARED EXPERIMENT (SIRE)

The objective of the SIRE program is to launch into orbit a highly sensitive infrared telescope to survey targets and backgrounds. The detector and its optics will be cryogenically cooled. (A NASA program, the Shuttle Infrared Telescope Facility, is similar in nature.) Deposition of contaminants upon the cooled optics can degrade the performance of the sensor. The sources of such condensates are the ambient atmosphere and the induced (outgassed) atmosphere of the satellite. It has been estimated that a cryodeposit that is only 1 μm thick will have a significantly deleterious effect.[12]

At 300 km, during periods of high solar activity, the density of atomic oxygen is about 10^9 cm^{-3}.[1-3] Assuming a unit sticking coefficient to produce solid O_2, one calculates that an exposed surface normal to the velocity vector of a spacecraft orbiting at 8 km sec^{-1} will accumulate O_2 at a rate of about 2×10^{-8} $g\text{-}cm^{-2}$ sec^{-1}, which corresponds to about 50 μm of deposit in only 1 hour. Such a rate of mass accretion is clearly unacceptable.

It has been suggested that an outward flow of helium or neon might prevent contamination of the primary mirror of the SIRE telescope by directing contaminants to other surfaces.[12,13] Approximate calculations of the efficiency of such a scheme have been performed, but a calculation incorporating a realistic model of each process involved in a purge flow to protect the telescope mirror has not yet been performed.[13]

5. DEFENSE METEOROLOGICAL SATELLITE PROGRAM (DMSP)

A degradation in performance of the ESA of the DMSP spacecraft and their sister craft from the National Oceanographic and Atmospheric Administra-

tion/Television and Infrared Observation Satellite (NOAA/TIROS) Program has been observed.[14] Timing of the degradation indicates that an interaction with atomic oxygen in the atmosphere may play a role in this degradation. This problem is discussed in detail in Section IV.

C. OXYGEN ATOM SURFACE CHEMISTRY

Because atomic oxygen is the most abundant specie in the atmosphere from 200 to 1100 km, the gas-surface chemistry of atomic oxygen and techniques for its investigation are discussed in the remainder of this section. A number of different processes may occur when an oxygen atom interacts with a surface, such as elastic scattering, inelastic scattering, reactive scattering with the surface or with some species deposited on the surface, occlusion (reaction with the solid phase), absorption-desorption, recombination into O_2, and sputtering of loosely bound surface materials.

Because of the difficulty of producing moderately high energy (2 to 10 eV) oxygen atoms in the laboratory, knowledge of high energy oxygen atom surface chemistry is severely limited. Indeed, a literature search produced no indication that any investigations of oxygen atom interactions with surfaces in the 2 to 10 eV range have ever been conducted. A number of experimental investigations of oxygen atom surface chemistry, at lower energies, are described in succeeding paragraphs to indicate the state-of-the-art in this area.

1. REACTIVE SCATTERING OF OXYGEN ATOMS FROM SURFACES

Madix and coworkers have investigated the oxidation of clean, single crystal surfaces of germanium and silicon by atomic and molecular oxygen.[15] In these experiments, atomic oxygen from an effusive beam source, whose most probable velocity was less than 1 km sec^{-1},[16] was directed upon heated surfaces of silicon and germanium. From the experimentally determined flux of oxygen atoms and from the observed rates of weight loss of the semiconductor crystals, the reaction probabilities, α_o, were determined. These probabilities were 0.15 to 0.5 for germanium surfaces between 800 and 1100 K, and 0.3 to 0.6 for silicon between 1300 to 1400 K. No dependence on surface temperature or wafer orientation was observed. These rates are an order of magnitude

19

greater than rates of oxidation for silicon and germanium by O_2. The sole products of these oxidation reactions have been observed to be the monoxides of silicon and germanium.[14] Liu has reported a molecular beam, mass spectrometric investigation of the reaction of atomic and molecular oxygen with graphite surfaces.[17] The source of atoms used in these experiments produces a most probable velocity of about 1.8 km sec^{-1}.[16,17] These experiments show that carbon monoxide is the dominant product of both atomic and molecular oxygen reaction with 1000 to 1700 K surfaces. The reaction probability for atomic oxygen under these conditions is 0.1 to 0.3, showing no simple or large dependence upon substrate temperature. These probabilities are greater than a factor of ten larger than those for molecular oxygen.

2. ELASTIC SCATTERING, INELASTIC SCATTERING, AND ATOM RECOMBINATION

Several measurements of the scattering of low energy ($E < 0.33$ eV) atomic oxygen from surfaces have been reported. Many of these studies have been performed with the goal of providing calibration data for mass spectrometers used in upper atmospheric measurements.[18-25] These studies focused on atomic oxygen losses on metal surfaces in mass spectrometer ion sources. Most of these studies report only loss coefficients, i.e., whether an oxygen atom impacting a surface will bounce off, or stick and recombine to form O_2.

Wood[26] examined the rates of adsorption, occlusion, and recombination of oxygen atoms on silver and gold surfaces. It was found that oxygen atoms react on clean silver surfaces by adsorption and occlusion and on gold surfaces by recombination. These experiments showed that silver (at 300 K) takes up atomic oxygen at a nearly constant rate well beyond monolayer coverage. The nature of the occluded state was not determined. The occlusion rate was measured to be 3.3×10^{14} atoms cm^{-2} min^{-1}. It was observed that gold adsorbs up to a maximum of one monolayer of oxygen atoms at 300 K with a rate that diminished with coverage.

Wood, Baker, and Wise[27] examined oxygen interactions with gold, silver, titanium, stainless steel, and aluminum surfaces. Oxygen was shown to be lost at gold surfaces by atom-adatom recombination. Occlusion was again shown to be the primary loss mechanism on silver surfaces. Titanium reacted with

oxygen atoms to form a variety of solid oxides in a manner so complex that kinetic measurements were not possible. Oxide-coated aluminum was virtually inert to oxygen atom reaction or recombination. The interaction of oxygen atoms with 302 stainless steel varied with pretreatment of the metal. In general, loss rates were greater for steel than for noble metals. Under certain conditions atomic oxygen reacted with carbon in the steel to form CO_2.[27]

Riley and Giese used atomic beam, mass spectrometric techniques to determine the probability of reflection of atomic oxygen from various surfaces, such as Pyrex, stainless steel, Teflon, gold, and aluminum.[28] They observed reflection probabilities to lie between 45 and 60% for all these materials at room temperature. The reflection probability for metals showed a strong, inverse temperature dependence dropping to below 10% at 673 K. (Such a dependence upon surface temperature may cause one to doubt the accuracy with which observations for these low energy collisions, < 0.33 eV, can be extrapolated to describe events occurring at orbital velocity, about 8 km sec^{-1}, that is about 5 eV.) The atoms which were not reflected in these experiments apparently stuck to the surfaces. There was no evidence of recombination or production of small molecules such as CO_2 or N_2O in experiments carried at 10^{-7} Torr.[28] Hollister, Brackman, and Fite have described techniques for beam-surface measurements of quantities of interest, such as reflection probabilities and thermal accommodation rates.[29]

3. REMOVAL OF SURFACE CONTAMINANTS BY NEUTRAL ATOM BOMBARDMENT

Discharge flow experiments carried out at Boeing Aerospace Co. have shown that ultraviolet polymerized contaminant films[30] can, in some cases, be removed by the action of radio-frequency excited oxygen.[31-33] Oxygen plasmas successfully cleaned ultraviolet polymerized hydrocarbons from various mirror and grating surfaces, silvered Teflon, and fused silica flats. Exposure to oxygen plasma further degraded hydrocarbon-contaminated thermal control paint samples. A synergistic effect is indicated by the fact that the oxygen plasma had no affect upon pristine samples of the paint. Oxygen plasmas could not remove silicon containing contaminants.

It was proposed that it was the oxygen atoms produced in the radio-frequency discharge that caused the contaminant cleaning. However, further experiments showed that a beam of radio-frequency excited O_2 was successful in cleaning hydrocarbon contaminants only when the contaminated surface was exposed to the luminescent plume of a discharge source. This suggested that ions, or some excited species contained in the luminescent plume, and not the oxygen ^3P atoms alone, were responsible for the cleaning.[34,35]

Sputtering of adsorbed species by neutral atoms has been observed in experiments on scattering of rare gas beams from a (111) silver surface.[36,37] Surface cleanliness of epitaxially grown silver, which became contaminated by hydrocarbon background gases in the molecular beam apparatus, was monitored before and after bombardment by a high energy argon atomic beam. A distinct threshold for contaminant sputtering of 1.0 to 2.0 eV (dependent upon angle of incidence of the atomic beam) was observed. This observed threshold for contaminant sputtering suggests that the failure to clean contaminants in the oxygen atom beam/surface experiments described above may owe to the collision energy in these experiments being below threshold. The velocity distribution of the oxygen atom beam of References 34 and 35 was not measured, but similar sources[38] produce velocities of 2 km/sec or less, or collision energies of less than 0.33 eV. One should note, however, that oxygen atoms impacting a satellite at orbital velocities have a collision energy of about 5 eV, which is well above the threshold observed for argon sputtering of contaminant films.

5. EFFECT OF ATOMIC OXYGEN ON POLYMERS

Experiments in which radio-frequency excited oxygen impinged upon thin films of polymers have shown that polymers can be rapidly oxidized by the active species in discharged O_2. Hansen et al. have studied oxidation of some three dozen polymers by exposure to 1 Torr of radio-frequency excited O_2.[39] Under their conditions the atomic oxygen concentration was of the order of 10^{14} to 10^{15} cm^{-3}, with flow rates of 4 cm^3 (STP)/min. All samples showed measurable weight loss, typically on the order of 60 $\mu g\text{-}cm^{-2}min^{-1}$. During oxidation, emission of light from excited O_2 and oxygen was observed, as well

as emission from oxidation products, depending on the polymer under attack. For example, CO_2 and OH emission was observed when hydrocarbon polymers, such as polyethylene were oxidized. SO bands, as well, were observed when sulfur-containing polymers were treated.

Bulk properties of the polymers were not affected by the attack of atomic oxygen, however, surface-dependent properties were affected. In many cases simple ablation of the polymer surface occurred during oxidation by atomic oxygen: polymeric material was simply oxidized and volatilized. Fluorinated polymers behaved in this manner. In other polymers, especially polyethylene and polypropylene, a hazy, oxidized surface layer was created. The oxidized surface layer was hydrophilic. The surface oxide layer has the characteristic of formation of strong adhesive bonds and provides sites for chemical attachment of other molecules.[40]

D.   EXPERIMENTAL TECHNOLOGY

In order to understand what physical and chemical effects may arise from atmospheric oxygen atom bombardment of spacecraft surfaces, laboratory investigations need to simulate that bombardment as closely as possible. In particular, the velocity at which the atoms impact the surface ought to be high, about 8 km sec^{-1}. This high velocity of impact results, on orbit, from the spacecraft sweeping rapidly through a more-or-less stationary atmosphere. Clearly, one may simulate this situation more readily in the laboratory by producing rapidly moving gaseous atomic oxygen, which in turn impacts upon a stationary surface. Such a simulation may most readily be performed by means of atomic beam techniques.

Common atomic beam sources fall into two major classifications: effusive and hydrodynamic (supersonic nozzle) flow sources.[41] An effusive source consists of a small chamber in which the beam material is contained. Atoms and molecules leave the chamber by way of a small slit or orifice. The gas pressure is controlled so that molecules and atoms leave by effusion rather than bulk flow. The most probable velocity, v_{mp}, of particles leaving such a source is given by

$$V_{mp} = \left(\frac{3kT}{M}\right)^{1/2} \qquad (1)$$

where M is the particle mass, k is Boltzmann's constant, and T is the absolute temperature. In order to obtain oxygen atoms at 8 km sec^{-1}, such a source must operate at over 40,000 K.

Higher velocities can be obtained by using hydrodynamic flow sources, in which a gas at relatively high pressure undergoes an isentropic expansion through a small nozzle. Relaxation during the gas expansion effectively converts source enthalpy into a directed flow velocity, V_o,

$$\frac{1}{2} \langle M \rangle \, V_o^2 \cong \int_o^{T_s} C_p dT \qquad (2)$$

where T_s is the source temperature, $\langle M \rangle$ is the average mass, and C_p is the heat capacity at constant pressure of the gas. If the atomic oxygen were diluted in helium, then $\langle M \rangle$ is approximately equal to that of helium, 4 g mole^{-1}. Thus to obtain 8 km sec^{-1} oxygen atoms from a source of this nature would require a T_s of 6000 K.

It is because of these high source temperatures required to generate 8 km sec^{-1} oxygen atoms that no one has yet reported in the literature such a source. Numerous lower velocity sources of oxygen atoms have been described. Nearly all rely on two basic techniques for producing oxygen atoms: AC discharges of gaseous mixtures containing O_2, or thermal dissociation of O_2 in hot gas mixtures. Several sources that may be considered as archetypes are described herein.

Gorry and Grice have used a 2450 MHz discharge to produce oxygen atoms in mixtures of O_2 in inert gases. This source operates at relatively high pressure, 90 to 200 Torr. At those pressures, flow from the source is hydrodynamic (or very nearly so). Depending upon source pressure, the oxygen atom velocity produced when He is the diluent peaks at 2.0 to 2.5 km sec^{-1}. Oxygen atom fluxes are about 5×10^{17} sr^{-1} sec^{-1}.

Sibener et al.[38a] have described a source in which oxygen atoms are produced in a radio-frequency (about 14 MHz) discharge. The source has been

operated at pressures above 200 Torr for mixtures of He and O_2 producing oxygen atom intensities > 5×10^{18} sr^{-1} sec^{-1}. The velocity distribution of this source peaked at 2 to 2.5 km sec^{-1}.

Liu[17] has reported a thermal dissociation source for the production of an effusive beam of oxygen atoms. His source consists of a thorium oxide tube which is wrapped with a tungsten filament. An AC current heats the filament, which in turn heats the tube to temperatures in excess of 2100 K. Application of kinetic theory[15] indicates that this source produces about 8×10^{14} sr^{-1} sec^{-1} of oxygen atoms, with a peak velocity of about 1.8 km sec^{-1}. Peplinski has described a source of similar performance in which a source tube of iridium is heated directly by an AC current.[43]

Extremely high atomic velocities have been produced in atomic beam sources by the use of high power (several kilowatt) DC arcs to heat source gases. Such devices have been successful in producing beams of rare gases,[37,44] nitrogen atoms,[45] and hydrogen atoms.[46,47] Velocities in excess of 9.8 km sec^{-1} for a binary mixture of Ar in He have been produced. However, the introduction of O_2 into such a discharge has resulted only in the rapid oxidation of the arc electrodes.[48]

A novel beam source in which a DC arc is used to heat a stream of He into which O_2 is injected (down stream of the arc) is under development. In this manner, one hopes to obtain the high source temperatures of a DC arc while avoiding the problem of electrode oxidation. Such a source under development at the Air Force Geophysics Laboratory has produced O_2 dissociation efficiencies indicative of gas temperatures of 3500 K.[49]

III. DEFENSE METEOROLOGICAL SATELLITE EARTH
SENSOR ASSEMBLY OFFSET ANOMALY

The DMSP of the Air Force tries to maintain at least two satellites in operation at all times in circular, sun-synchronous, polar orbits at an altitude of 830 km. It provides U.S. military users with twice-daily global and limited local, near-real-time cloud cover and Earth surface imagery and information on atmospheric conditions.

In October 1978, one flight (F-3) of the DMSP Block 5D/1 lost Earth stabilization because one of the space viewing detectors in its ESA was showing an unexpectedly high count rate, a rate above the preset 900 count limit.[14] When the ESA drifted above the 900 count limit, the spacecraft control subsystem assumed that it had lost its lock on the Earth and initiated an automatic Earth reacquisition cycle. After a brief stabilization, the spacecraft again lost Earth stabilization. This sequence of events continued until the detector limit was reset to a higher level, 1200 counts. Such an effect has been observed on other DMSP Block 5D/1 flights and on similar satellites.

A. EARTH SENSOR ASSEMBLY

The ESA is a static infrared horizon sensor that provides pitch and roll data for the determination and control of spacecraft attitude (Fig. 2). These data are used as a monitor of and backup for the primary attitude control system on the DMSP satellites. The ESA is the primary attitude sensor for NOAA/TIROS spacecraft. The operation of the ESA, in particular those elements germane to the ESA offset anomaly, is described herein.[50]

The ESA has four detector arrays, which observe the Earth's limb, as shown in Fig. 3. Each array consists of four thermopile detectors sharing a common objective lens. Bandpass filters limit detector sensitivity to the 14 to 16 μm range. The detectors labeled A and B observe CO_2 ν_2 emission from the atmosphere, whereas those labeled S provide a background reference. The simple geometric relationship[50] between the A and B fields of view establishes the horizon with respect to each of the four detector assemblies.
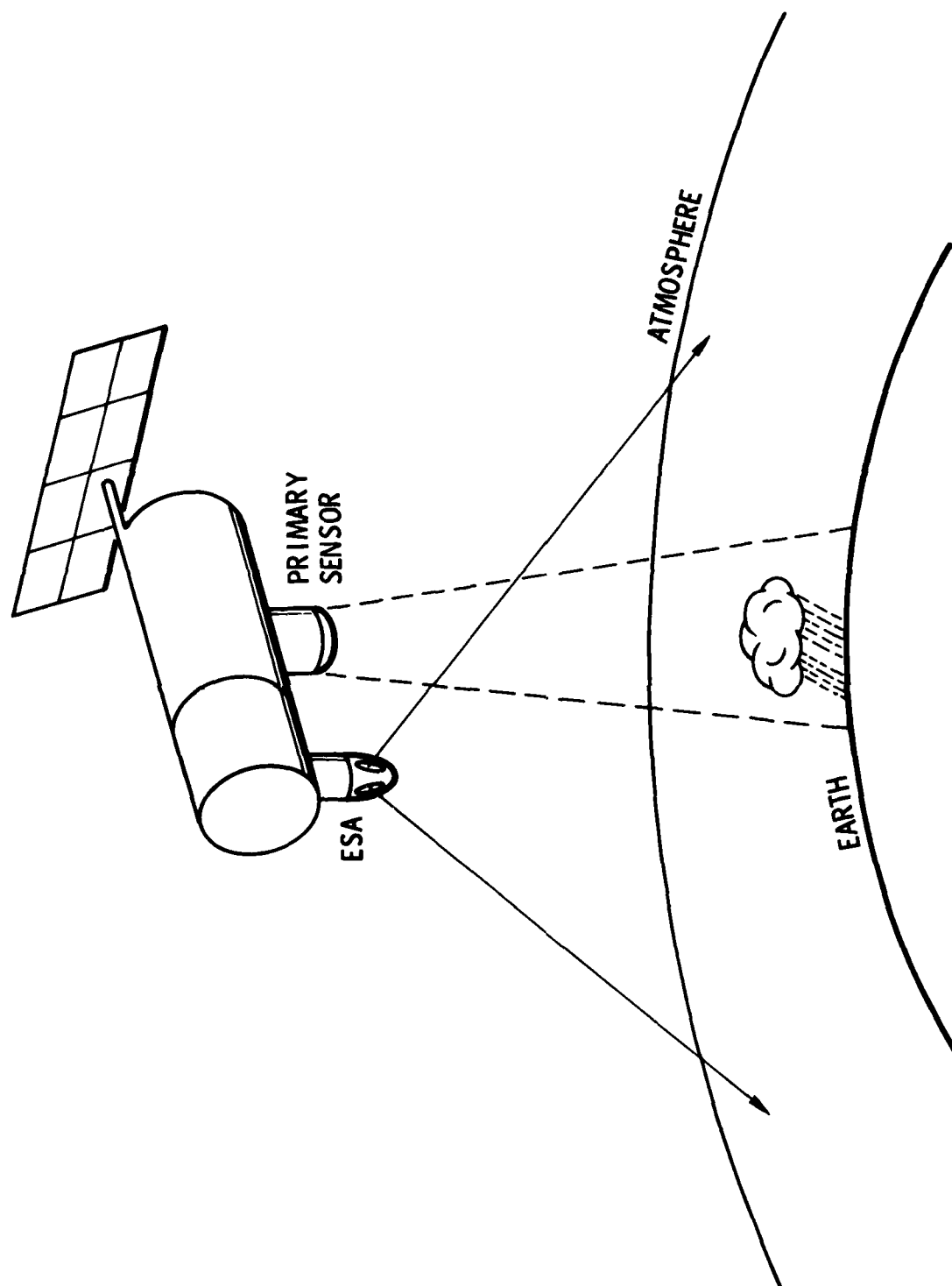
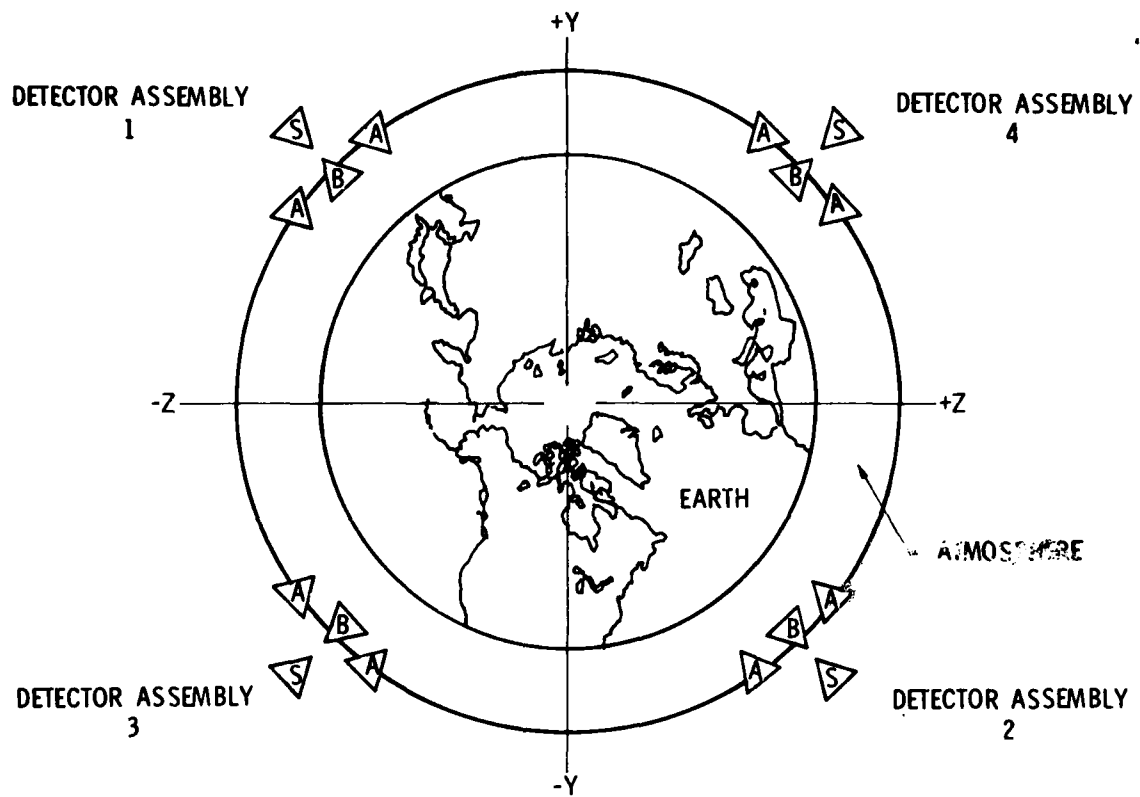Fig. 2.   Schematic Representation of a DMSP Satellite in Flight

Fig. 3.   ESA Fields of View

The active junctions of the thermopile detectors viewing cold Earth or space radiate heat and thus become colder than their reference junctions. This produces a large negative background signal upon which small horizon signals must be detected. This background negative signal is removed by subtracting the output of the space viewing detector (S) from those of the horizon viewing detectors (A and B). Because the responsivities of the detectors are not perfectly matched, the magnitude of this correction is reduced by using an offset radiation source (ORS) to compensate for heat lost to space by the detectors. The ORS is a heated IRTRAN 2 ball, which emits poorly at wavelengths shorter than 12 μm. Radiation from the ORS is focused onto all detector elements. The intensity of the ORS is regulated to drive the most negative S detector to a predetermined value, near zero.

The four objective lenses of the ESA are also its windows. The f/1.7 germanium lenses are 59 mm in diameter. Their front surfaces are coated, Optical Coating Laboratories, Inc. (OCLI), to reflect solar radiation from 0.4 to 2.4 μm. The rear surface is coated to reflect solar radiation and block transmission from 1.8 to 12 μm.

B.   ESA DEGRADATION

Four satellites have been orbited in the DMSP series 5D/1. Launch dates for these craft are shown in Table 3. Although the increase in count rate (henceforth known as degradation) was not observed until flight 5D/1 F-3, it has since been observed on all four satellites.[14] The same effect has been observed on two NASA satellites TIROS-N and NOAA-A. (Those satellites perform a function similar to that of DMSP. They fly circular orbits of 870 km, slightly higher than DMSP.)

The greatest degradation rate for the 5D/1 F-1 and TIROS-N ESAs occurred in February 1979. The 5D/1 F-3 showed a maximum degradation rate in October 1978.[14] Flight 2 also showed degradation, however, the exact timing of the maximum degradation is unknown because of other problems. It appears, however, that all degradations occurred within a few months of one another.[5] (Degradation of 5D/1F-4 began immediately after launch.) The detector assemblies that were front facing, i.e., facing into the wind or ram direction

30

Table 3. DMSP Block 5D/1, TIROS-N, and NOAA-A Satellite Launch Dates and Degradation Extent

Flight	Direction of Flight[a]	Launch	ESA Quadrants Affected (and Relative Extent of Degradation)
F-1	+Y	September 11, 1976	Q1 (0.37)
F-2	+Y	June 4, 1977	Q1 (0.32), Q4 (0.042)
F-3	+Y	May 1, 1978	Q1 (1), Q4 (0.10)
F-4	-Y	June 6, 1979	Q2 (0.63), Q3 (0.89)
TIROS-N	-Y	October 13, 1978	Q2 (0.23) Q3 (0.26)
NOAA-A	-Y	June 24, 1979	Q2 (0.04) Q3 (0.03)

[a]See Fig. 3

31

experienced the most degradation. However, there is some later evidence,[51] which indicates that the rear detector assemblies also degraded, but to a lesser extent (10 to 20% of the front facing detectors). Although degradation was most immediately apparent in the S detectors, the offset occurs equally in all four detectors of an affected quadrant. This fact was confirmed when quadrant 1 of DMSP F-3 viewed space with all channels during an Earth requisition sequence.[52]

C. NIMBUS 6 AND 7 ERB INSTRUMENT

NIMBUS 6 was launched in June 1975 into an 1100 km high sun-synchronous, polar orbit. NIMBUS 7 was launched in October 1978 into a 925 km high sun-synchronous polar orbit. The Earth Radiation Budget (ERB) experiment was designed to provide highly accurate radiation measurements of the sun and Earth. The measurements were designed to serve as a benchmark data set for the long-term monitoring of the radiation of the global environment. Measurements of radiation were made with 22 thermopile detectors with appropriate filters. Ten of these spectral channels measured ultraviolet and visible incoming solar radiation as the satellite orbited over the Antarctic. The remaining channels measured Earth radiation in the 0.2 to 50 µm region.[53]

The ERB instrument is mounted on the forward or ram side of the spacecraft. Four solar channels (6,7,8, and 9) of NIMBUS 6 showed a slow continuous drop in apparent solar radiance over 3 years. A drop in apparent solar radiance (in channels 6 to 9) began on the first day of observations on NIMBUS 7. These decreases in detected solar radiance apparently result from contamination of the solar channels by outgassing products of the spacecraft.[14]

The signal from the affected ERB channels of NIMBUS 6 began gradually to increase in October 1978. Early in 1979 these signals increased rapidly. The decay in signal on channels 6 to 9 of NIMBUS 7 reversed in January 1979, and the signal then increased rapidly to a value greater than that observed when measurements were begun. These affected channels faced into the atmospheric wind; solar radiance observations made by rear facing detectors on NIMBUS 7 showed no such rapid fluctuations. This apparent rapid, uncharacteristic

clean up of contamination of the ERB instruments occurred during the same period of time that degradation of the DMSP and NOAA/TIROS ESAs was occurring.

D.   DEGRADATION MECHANISMS

There is strong evidence that the ESA offset is caused by a decrease in the transmission of the objective lenses of the affected quadrants, which reduced the radiative heat loss from the detectors.[52] The agent causing such a decrease in transmission must affect the 14 to 16 μm region of the spectrum in which the ESA lens is transparent, but its effects need not be limited to this region. Such an effect would also lower the apparent Earth radiance as measured by the ESA. An analysis of the radiance measurements from quadrants 1 and 3 of DMSP F-3 before and after ESA degradation shows just such a reduction. The decrease in transmission necessary to explain both the detector offsets and the reduced apparent radiance is of the order of 20%.[52]

Optical Coating Laboratories, Inc., has performed calculations to determine what alterations to the outer coating of the ESA objective lens are necessary to account for a 20% decrease in transmission.[54] Physical removal of coating material as deep as 50% of the second layer does not radically alter the transmission around 15 μm. The effects of deposition of films of various thickness with an index of refraction of 1.6 and of various optical absorption coefficients (β) have been calculated. The results of these computations are shown in Table 4.

Although these calculations by OCLI indicate that a contaminant layer of great optical thickness in the long-wavelength infrared would be necessary to produce the required 20% decrease in transmission, an induced opacity of the lens remains the best explanation of the observed behavior of the ESA. That the effect on all detectors of a degraded quadrant was the same tends to rule out degradation of the detectors themselves or of optical elements unique to a particular detector. A change in the ORS output alone would not account for a decrease in the observed Earth radiance. Solar heating of the ESA is not indicated since the offset appears both on ESA quadrants whose objective lenses view the sun and on those which do not. Finally, electronic problems in reading the detectors or communication are not indicated, inasmuch as the effect is observed when either of two redundant sets of electronics is used.

Table 4. 15.0 μm Transmission of ESA Objective[54] Lens Coating with Various Layers of Contamination[a]

OWTO[b] (μm)	Thickness (nm)	β = 0	β = 10^2 cm^{-1} (3.3 × 10^{-20} cm^2)[c]	β = 10^3 cm^{-1} (3.3 × 10^{-19})	β = 10^4 cm^{-1} (3.3 × 10^{-18})
0	0	0.951	0.951	0.951	0.951
0.1	15.6	0.950	0.947	0.945	0.927
0.5	78.1	6.940	0.940	0.930	0.847
1.0	156	0.928	0.825	0.909	0.760
5.0	781	0.833	0.825	0.763	0.383
10	1563	0.764	0.754	0.667	0.200
15	2344	0.79	0.773	0.653	0.100
20	3125	0.90	0.869	0.677	0.047
25	3906	0.95	0.91	0.64	

[a] n = 1.6
[b] Quarter wave optical thickness = 4 nt
[c] Assumes a molecular weight of 200 amu and density of 1.0 g-cm^{-3}

34

That the greatest degradation rates for the DMSP and NOAA/TIROS ESAs occurred simultaneously with the restoration of the NIMBUS solar channels suggests that there may be a single cause for these phenomena. Any proposed mechanism for these processes must explain this coincidence and explain why the effects occur predominantly on surfaces facing in the ram direction.

R. Predmore has considered several degradation mechanisms.[14] The data he has accumulated indicate that because of the spacecraft geometries, the ESA degradation could not be explained by condensation of spacecraft outgassing material alone. The effect of high energy charged particles (protons, electrons, and alpha particles) has been ruled out because no increase in the density of such particles occurred during the time of interest and because the effect of such high energy particles would be omnidirectional. The possible effects of the CAMEO experiment carried aboard NIMBUS 7, which released 38 kg of lithium and barium at the end of October 1978, were also shown to be negligible.[14]

The anisotropy of the effects upon the ESAs and ERBs suggests the possibility that interaction with atmospheric constituents may play a role in the observed degradation. During the period in which rapid variations were observed by the ESAs and ERBs there was an increase in solar activity, which strongly affected the concentration of atomic oxygen and singly ionized oxygen at the orbital altitude of the affected satellites. Predmore[14] reports a calculation performed by Hedin, which gives the oxygen atom concentration variation in 1978 and 1979 at an altitude of 800 km. The oxygen atom concentration peaked in January and February 1979 and is reported to be the highest concentration in over 20 years. A more recent calculation[51] by L. T. Greenberg of the Optical Systems Department at Aerospace places the peak in oxygen atom concentration somewhat later, in March 1979.

Assuming an orbital velocity of 8 km/sec, DMSP experiences bombardment by an oxygen atom flux of about 10^{12} cm^{-2} sec^{-1} at sunspot maximum. Figure 4 shows a plot of the ESA degradation observed as a function of time.[14] Also plotted is the integrated oxygen atom flux.[51] The increase in the lower O^+ concentration takes the same form. In general, the failed detectors suffered an oxygen atom integrated flux of about 10^{19} cm^{-2}.
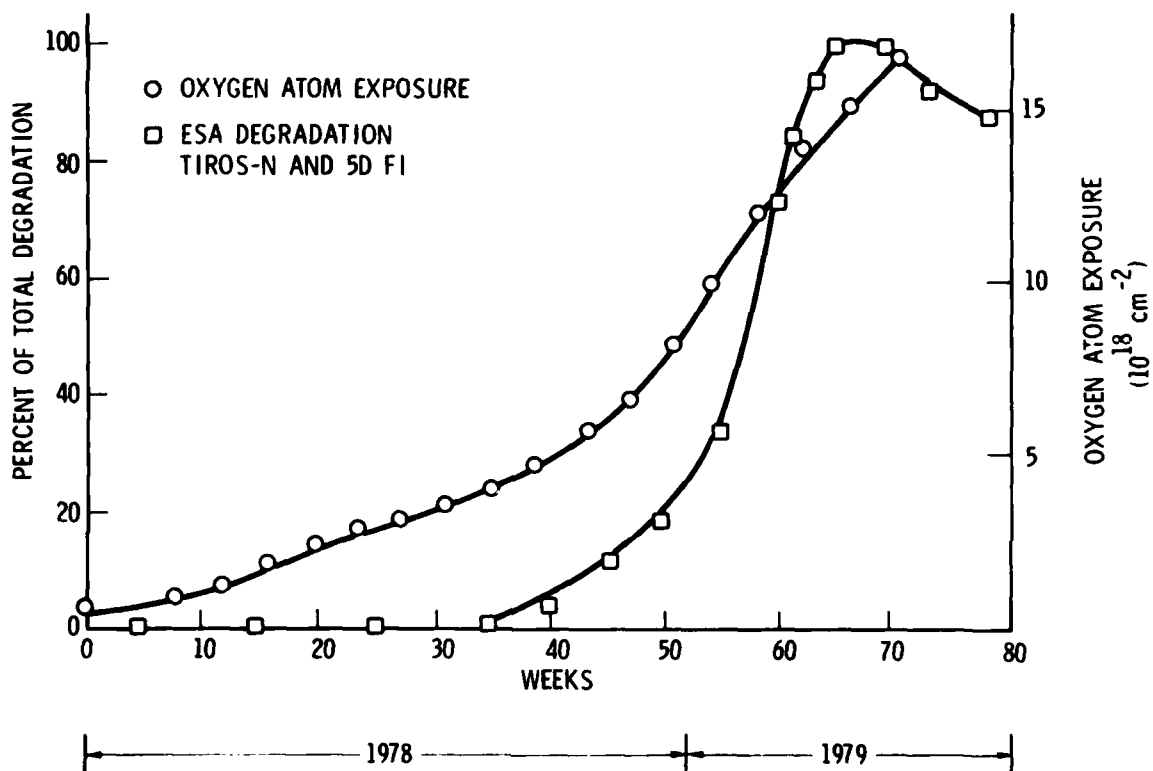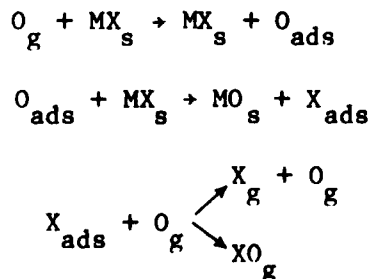
Fig. 4.   ESA Degradation and Oxygen Atom Exposure as a Function
            of Time

Although this collection of observations is by no means conclusive, they suggest that the atmospheric fluxes of O and O^+ may play a role in the cleaning of the ERBs and the degradation of the DMSP, TIROS, and NOAA ESAs.

It is instructive to consider whether, in light of the OCLI calculations, it is physically possible for 10^{19} cm^{-2} of oxygen atoms to produce a 20% drop in the transmission of the ESA objective lens. The density of solid oxygen, 1.43 g-cm^{-3}, indicates the scale of the question at hand. If one assumes the admittedly unrealistic situation that each atom of oxygen striking the DMSP ESA lens (which is at approximately 10°C) condenses to form solid oxygen, 10^{19} cm^{-2} of oxygen atoms would form a layer 1.9 μm thick. Some situations, which are physically somewhat more reasonable, are examined herein.

One might assume that oxygen atom bombardment of the lens maintains an adsorbed layer of oxygen atoms, which migrate into the lens material by physical diffusion, thus altering the refractive index of the coating material. The period over which degradation occurred on DMSP F-3 was approximately 10 weeks. In order to produce a significant penetration of oxygen atoms as deep as 1 μm into the coating, the diffusion constant for oxygen atoms in the coating material would need to be of the order of 10^{-16} cm^2 sec^{-1}. This value is unreasonably large for a diffusion constant in a solid at or about room temperature.[55]

Although diffusion of oxygen atoms into the surface is unlikely, reaction of oxygen atoms with the surface material is conceivable. Calling the outer coating material MX, one may propose a reaction scheme as follows:[*]

$$O_g + MX_s \rightarrow MX_s + O_{ads}$$

$$O_{ads} + MX_s \rightarrow MO_s + X_{ads}$$

$$X_{ads} + O_g \begin{cases} \nearrow X_g + O_g \\ \searrow XO_g \end{cases}$$

_____

[*]The identity of the outer coating material is known to the authors, however, the manufacturer considers this information confidential.

The molar volume of MO is smaller than that of MX so it is reasonable to expect that the oxide layer formed will be porous and, therefore, the rate determining step may be the chemical process occurring at the interface.[56] This results in a rate determined by the exposed area of MX rather than by diffusion. If the mechanism proposed above (which is substantially exothermic at room temperature) were to occur at unit probability, a layer of MO approximately 1.2 μm thick could be generated.

A likely cause for the degradation of the ESA lens is the deposition of some spacecraft outgassing material whose ill effects are exacerbated by the incident atmosphere.[14,51] More than one role for the atmospheric flux is possible. A return flux of material outgassing from the satellite could be created by collisions with the incoming atmosphere. Impact of atmospheric atoms and molecules could produce a new source of outgassing material, which finds its way to the lens. Reaction of atmospheric oxygen with material on the lens could alter the surface so as to enhance the probability of satellite outgassing impurities sticking and remaining on the lens. Atmospheric oxygen may react with already deposited contaminants or those being deposited to produce a new species, which is more opaque in the 14 to 16 μm region.

Of these possible mechanisms, only the creation of a return flux by atmospheric impact really admits to critical examination. If one assumes a contaminant with a molecular weight of 200 and a specific gravity of 1.0, a 1 μm layer would be comprised of about 3×10^{17} cm^{-2} of molecules. If this material were deposited over the period of degradation of the DMSP 5D/1 F-3 ESA, the average flux of adhering contaminant molecules must have been 5×10^{10} cm^{-2} sec^{-1}. A reasonable estimate of the ratio of contaminant flux returned by atmospheric impact to the emitted flux of a spacecraft at the altitude of DMSP is 10^{-5}.[57] Thus if the build up of a 1 μm layer of contaminant by atmospherically induced return flux were the cause of the ESA degradation, the satellite must have been outgassing (under the assumptions of molecular weight and density proposed above) at the unreasonably high[38] rate of 1.7 μg-cm^{-2} sec^{-1} for 10 weeks.

E. DMSP ESA OFFSET ANOMALY LABORATORY EXPERIMENT

In order to test the hypothesis that atmospheric oxygen contributes to the ESA degradation, a molecular beam experiment was undertaken to simulate the neutral oxygen atom bombardment experienced by the DMSP spacecraft. The experiment was designed to determine the effect of oxygen atom bombardment upon the transmission of dielectric-coated germanium optics. This matter must be addressed experimentally inasmuch as the available knowledge of oxygen atom surface chemistry is insufficient to indicate what that effect might be.

The level of effort of this program and the time in which results were sought dictated that we rely upon proven atomic beam source technology. Thus, the impact velocity of the simulated oxygen atom bombardment of the satellite optics was limited to less than 2.5 km sec^{-1}, not the 6 to 8 km sec^{-1} experienced on orbit.

A positive result from such an experiment, that is, the observation of a decrease in the transmission of the optic resulting from oxygen atom bombardment, would strongly support the chemical degradation mechanism. A completely successful experiment would allow one to determine the relative importance of direct reaction with the surface and of reaction with some satellite contaminant and would thus indicate areas of effort for preventing such problems in the future. However, because the experimental bombardment takes place at a velocity one third of that encountered on orbit, a negative result would not conclusively disprove the hypothesis of atmospheric degradation of the performance of the optic.

The apparatus with which this experiment was performed is described in detail in Section IV. The results of the program are presented and discussed in Section V.

39

IV. EXPERIMENTAL APPARATUS

A schematic of the atomic beam apparatus used to test the chemical degradation mechanism for the DMSP ESA is shown in Fig. 5. The major elements of the facility are: a three chambered, differentially pumped vacuum system; a source of oxygen atoms; a mass spectrometer to characterize the beam source; a sample with a cryogenically cooled shroud to protect it from spurious contamination; and a light source and detector to monitor transmission of the sample at or about 15 μm. Each of these elements is described in more detail below.

A.   VACUUM SYSTEM

The basic vacuum chamber consists of three stainless steel boxes, 18 in. cubed. The first and third chambers are pumped by 10 in. oil diffusion pumps, Consolidated Vacuum Corporation (CVC) and the second by a 6 in. oil diffusion pump (CVC). Each pump is topped with a liquid nitrogen-cooled baffle (Mount Vernon Research Co.). Each chamber may be isolated from its baffled pump by means of an electropneumatically actuated, viton-sealed gate valve (Vacuum Research Manufacturing Co.). The approximate pumping speeds of the 6 and 10 in. pump-baffle-valve stacks are 750 and 1500 l/sec, respectively. The pumping fluid for chambers 1 and 2 is Dow Corning 704 silicon diffusion pump oil. A hydrocarbon oil, Santovac 5, is used in chamber 3 to provide a cleaner environment. The backing pump for chamber 1 is a 516 cfm Roots blower (Penwalt Corp., Stokes Equipment Div. No. 1718). Chambers 2 and 3 are backed in parallel by two mechanical pumps (Balzers DU090, 54 cfm and Sargeant-Welch 1397, 17.7 cfm).

Chamber 1, the source chamber, is extended into chamber 2 and through the top of chamber 2 (see Fig. 5). The purpose of this extension is to allow the beam source to be mounted as near as possible to the third chamber in which the bombardment occurs and thus to deliver the maximum available flux of oxygen atoms to the surface. A nickel skimmer (Beam Dynamics, Inc., Model 2) with an orifice diameter of 0.90 mm connects chambers 1 and 2.
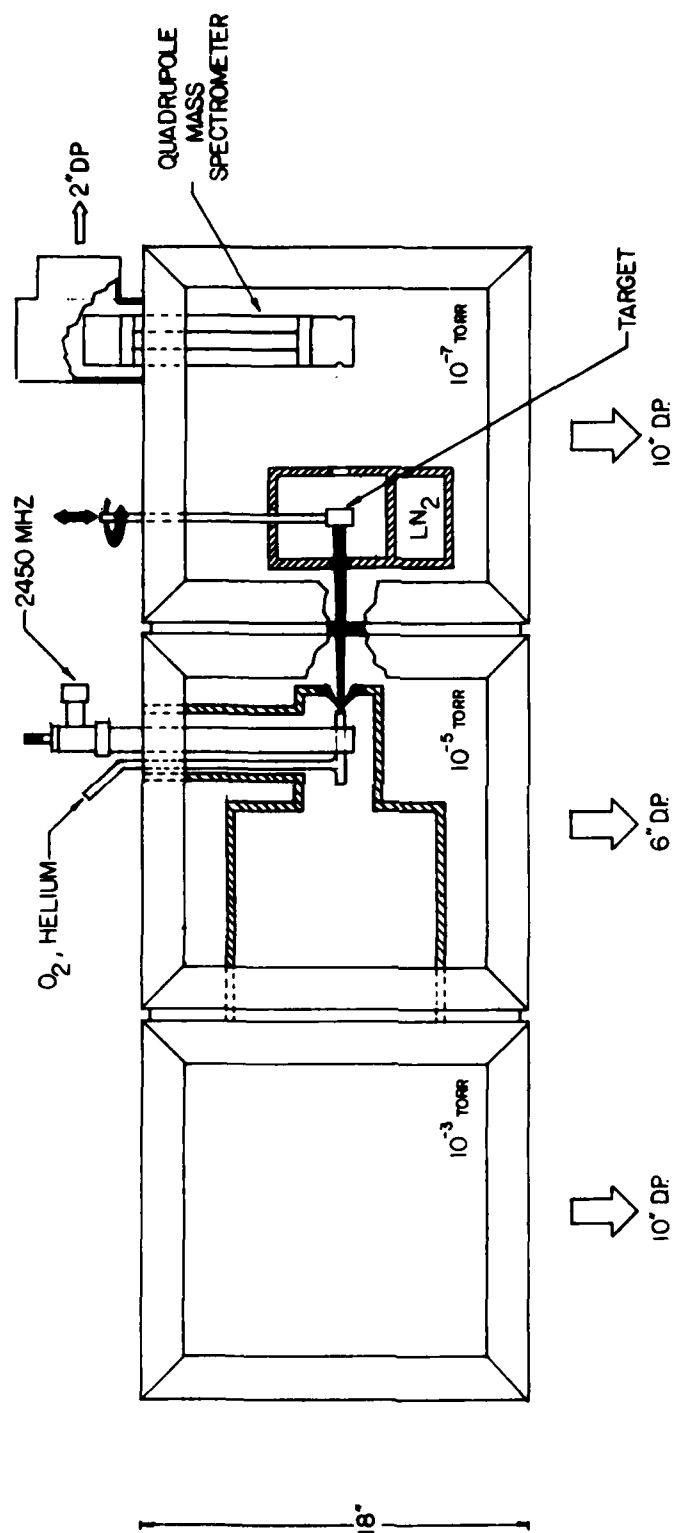
Fig. 5. DMSP ESA Laboratory Experiment Apparatus

Chamber 2 acts as a buffer to aid in the reduction of pressure between the source and the experimental chamber. Also mounted in chamber 2 are a beam chopper and a beam flag to aid in the characterization of the atomic beam (see below). The orifice connecting chambers 2 and 3 is a 2.4 mm diameter hole punched in a piece of stainless steel shim stock.

Chamber pressures are monitored by thermocouple gauges and by Bayard-Alpert-type ionization gauges. With no gas flowing through the source, the system pumps down to about 2.5×10^{-7} Torr. Source operating conditions are generally selected to keep the ionization gauge reading in chamber 1 < 1×10^{-3} Torr. Under these conditions the pressures in chambers 2 and 3 are about 1×10^{-5} and 3×10^{-7} Torr, respectively.

B. ATOMIC BEAM SOURCE

Oxygen atoms are produced by inducing a microwave discharge in gas mixtures containing O_2, and allowing the discharged gases to expand into the vacuum system to form a molecular beam. The source constructed for this experiment uses a cavity very similar to that described in detail by Murphy and Brophy.[59] The cavity is a 3-1/4 wave foreshortened coaxial type with microwave power coupling and cavity tuning of the Evenson design.[60] (A recent review[61] of microwave-supported discharges by Zander and Hieftje provides descriptions of various discharge cavities.) Power is supplied by a Raytheon PGM-10 2450 MHz magnetron power supply. The discharge tube is fused silica with a 1-mm-diameter orifice. Figure 6 shows a schematic of the discharge beam source.

Beam composition is measured with a quadrupole mass spectrometer (Extranuclear Laboratories.) The major elements of the spectrometer are a cross-beam, electron-impact ionizer including ion focusing optics, a quadrupole mass filter with 17 mm diameter rods, and an electron multiplier (Johnson MM-1). The electron multiplier signal is fed to an Extranuclear Laboratories 032-4 preamplifier whose output can be displayed on an oscilloscope, digital voltmeter, X-Y recorder, or lock-in amplifier.

In order to discriminate mass spectrometer signals for oxygen in the molecular beam from those for oxygen present as residual gas in the vacuum

43
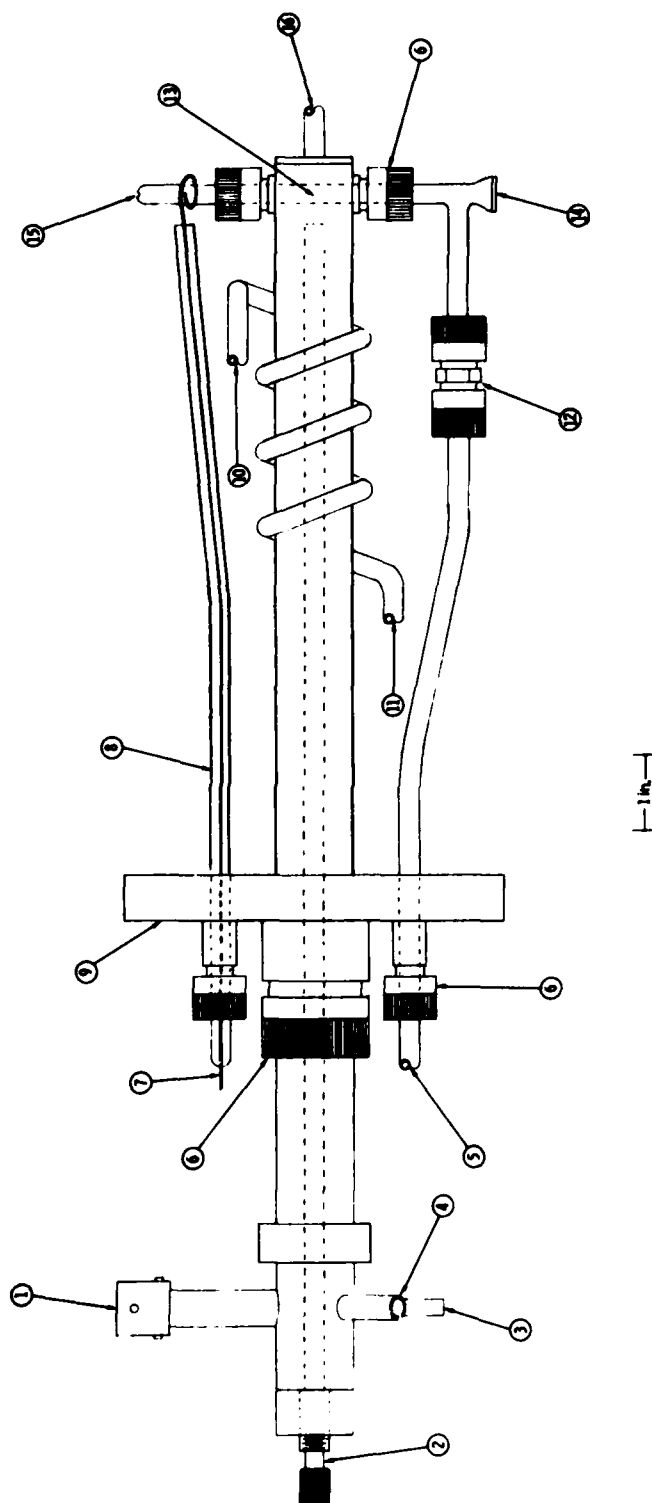
1. MICROWAVE POWER CONNECTION
2. CAVITY TUNING STUB
3. COUPLING TUNING STUB
4. COOLING AIR OUTLET
5. DISCHARGE GAS INLET
6. CAJON ULTRA-TORR FITTING
7. IGNITION ELECTRODE
8. PYREX MOUNTING FLANGE

9. SOURCE MOUNTING FLANGE
10. COOLING WATER INLET
11. COOLING WATER OUTLET
12. CAJON ULTRA-TORR UNION
13. DISCHARGE TUBE
14. WINDOW (to aid alignment)
15. ORIFICE
16. COOLING AIR INLET

Fig. 6.   Microwave Discharge Atomic Beam Source

system, the phase sensitive detection method is used. A two-bladed rotary chopper mounted in chamber 2 modulates the molecular beam at 47 Hz. A PAR Model 186 lock-in amplifier is used to detect the modulated beam signal. Figure 7 shows DC and AC mass spectra of the molecular beam.

The discharge source was operated with various gas compositions, source pressures, and microwave power levels to determine those conditions most suitable for performing the experiment. Conversion of oxygen into atoms was determined from relative mass peak signals, I_0/I_{O_2}, by the formula of Miller and Patch[38b]:

$$y = \frac{n_0}{n_{O_2}} = P \left(\frac{\sigma_{O_2}}{\sigma_0}\right) \left[\frac{1}{n} \frac{I_0}{I_{O_2}} - 1\right] \tag{3}$$

where P is the probability of dissociative ionization, (σ_{O_2}/σ_0) is the ratio of ionization cross sections, and $n = I_0/I_{O_2}$ with the discharge turned off. Values of P and σ_{O_2}/σ_0 are taken to be 0.30 and 1.30, respectively.[38b] The effective percent dissociation (%D) is equal to $100y/(y+2)$. Percent dissociations measured for pure O_2, and for 4.88, 9.79, and 14.35% O_2 in He all showed a dependence on source pressure with a maximum dissociation of about 20 to 30%. When a small amount of water was added to the gas flow by bubbling the feed gas through distilled, deionized water at 23 psi, the dissociation increased dramatically, as has been reported in the literature,[62] to a value of 50 to 60% for all three He/O_2 mixtures. The percent dissociation increased with microwave power coupled into the cavity. Figure 8 shows the dependence of %D on source pressure for gas mixtures containing O_2 in He.

It was determined that operating the source at 90 to 100 W with 18 to 20 Torr of 9.79% O_2 in He, saturated with water at 23 psi at room temperature, provided the best compromise between the requirement of maximum obtainable beam intensity and the limitations on microwave power and chamber pressure. Under these conditions the flux of oxygen atoms at the detector was estimated by comparing height of mass peaks arising from the beam to those in the residual gas to be 4 to 7 $\times$ 10^{14} cm^{-2} sec^{-1}. The beam flux decreases with the square of the distance from the source. Thus the flux of oxygen atoms bombarding a sample is four times greater than that observed at the
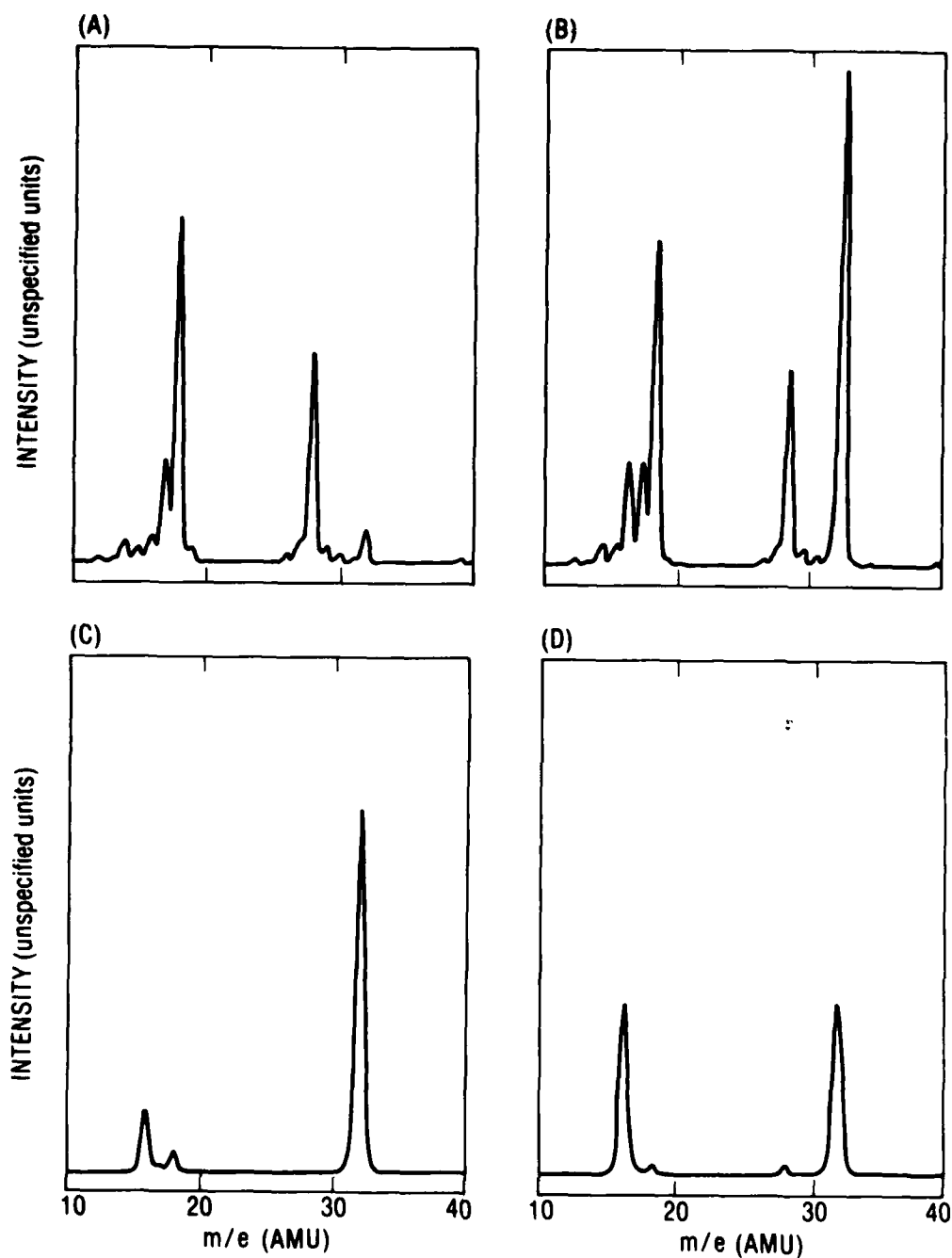
Fig. 7.   Mass Spectra of Oxygen Atom Beam. (a) DC spectrum,
            background gas; (b) DC spectrum, beam plus back-
            ground, discharge off; (c) AC spectrum, discharge
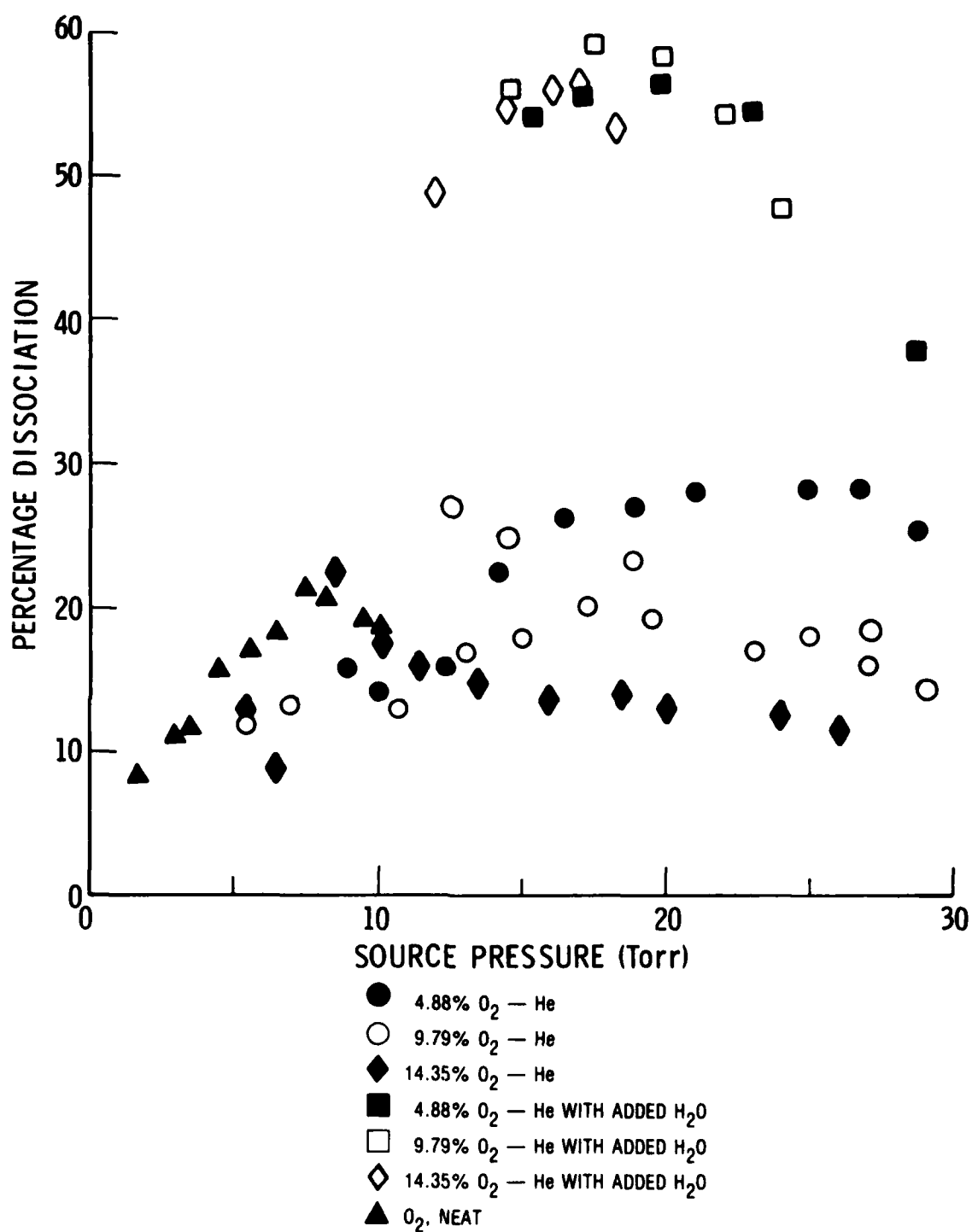   off; and (d) AC spectrum, discharge on.

46

Fig. 8. Pressure Dependence of O_2 Dissociation

detector. (See Fig. 5.) Therefore with these standard beam conditions, the 10^{19} cm^{-2} bombardment experienced by the DMSP spacecraft could be produced in less than 2 hr. Somewhat longer bombardment times were used in practice because of the approximate natures of the 10^{19} cm^{-2} figure and of the source flux calibration.

As well as producing atoms, the discharge emits light strongly. Emission owing to H, He, OH and O were observed in the discharge. Table 5 lists the various lines observed between 300 and 700 nm and their relative intensities under three different source conditions.

C. SAMPLE SYSTEM

Samples bombarded were various dielectric-coated germanium disks (25 mm o.d. × 1 mm thick) manufactured by OCLI. These samples were selected (except in the case of the final experiment, see below) to have the same outermost coating material as the ESA objective lens. The germanium flats were held between viton O-rings in a 304 stainless steel block. The temperature of the sample holder was controlled by two 10 W cartridge heaters (Hotwatt, Inc.), which were regulated by an Omega Model 49 temperature controller. The sample could be moved vertically (in and out of the beam path) and rotated about its vertical axis, with the system evacuated.

The sample was surrounded by a 76 mm o.d. copper cylinder, closed at the top and bottom, which was cooled to 77 K by liquid nitrogen. The purpose of this shroud was to protect the sample from contamination by condensible residual gases. Two openings of 6 mm diameter allow the atomic beam to pass through the cryoshroud. Two more openings at right angles to the beam path provide a path for spectroscopic interrogation of the sample.

Transmission of the sample between 14 and 16 μm was measured using a glow-bar light source, collimated with a 51 mm diameter, 76 mm focal length KCℓ lens. The detector was an Infrared Associates HCT 14-16 mercury-cadmium-telluride photoconductive detector. The detector was protected with a 14 to 16 μm band pass filter, OCLI 15000-9A. A 200 Hz Bulova tuning fork chopper modulated the probing light, and the detector signal was monitored by a PAR 186 lock-in amplifier. Figure 9 shows a schematic representation of the optical system.

48

Table 5. Emission Lines Observed from Microwave Discharge
Beam Source Under Various Conditions

Wavelength (nm)	Assignment	Intensity (arbitrary units)		
		He[a]	He: O_2H_2O[b]	O_2[c]
668	He $^1P°$ – ^1S	387		
656	H Balmer α	26	165	5
654	d		2	1
588	He $^3P°$ – ^3D	1000	14	
505	He $^1P°$ – ^1S	9		
502	He ^1S – $^1P°$	259		
492	He $^1P°$ – ^1D	90		
486	H Balmer β	5	26	
476	d		144	
471	He $^3P°$ – ^3S	47		
447	He He$^3P°$ – ^3D	267		
439	He $^1P°$ – ^1D	13		
436	d		5	
434	H Balmer γ		4	
414	He $^1P°$ – ^1D	2		
412	He $^3P°$ – ^3S	6		
403	He $^3P°$ – ^3D	40		
397	(H Balmer δ)[e]		1	
396	He ^1S – $^1P°$	22		
389	He ^3S – $^3P°$	533		
382	He $^3P°$ – ^3D	6		
335	(He ^3S – $^3P°$)[e]	16		
319	d	64		
300 – 310	OH $X^2π$ – A^2E		18	1

[a]16.5 Torr, discharge 85 W
[b]Standard beam, see text
[c]8.5 Torr, discharge 100 W
[d]Unidentified
[e]Assignment uncertain

A. GLOWBAR LIGHT SOURCE

B. KCℓ LENS

C. IRIS

D. KCℓ WINDOW

E. COPPER CRYOSHROUD (77 K)

F. SAMPLE (298 K)

G. VCM SOURCE (398 K)

H. ATOMIC BEAM AXIS

I. QUADRUPOLE MASS SPECTROMETER

J. CHAMBER NO. 3

K. BANDPASS FILTER

L. HgCdTe DETECTOR

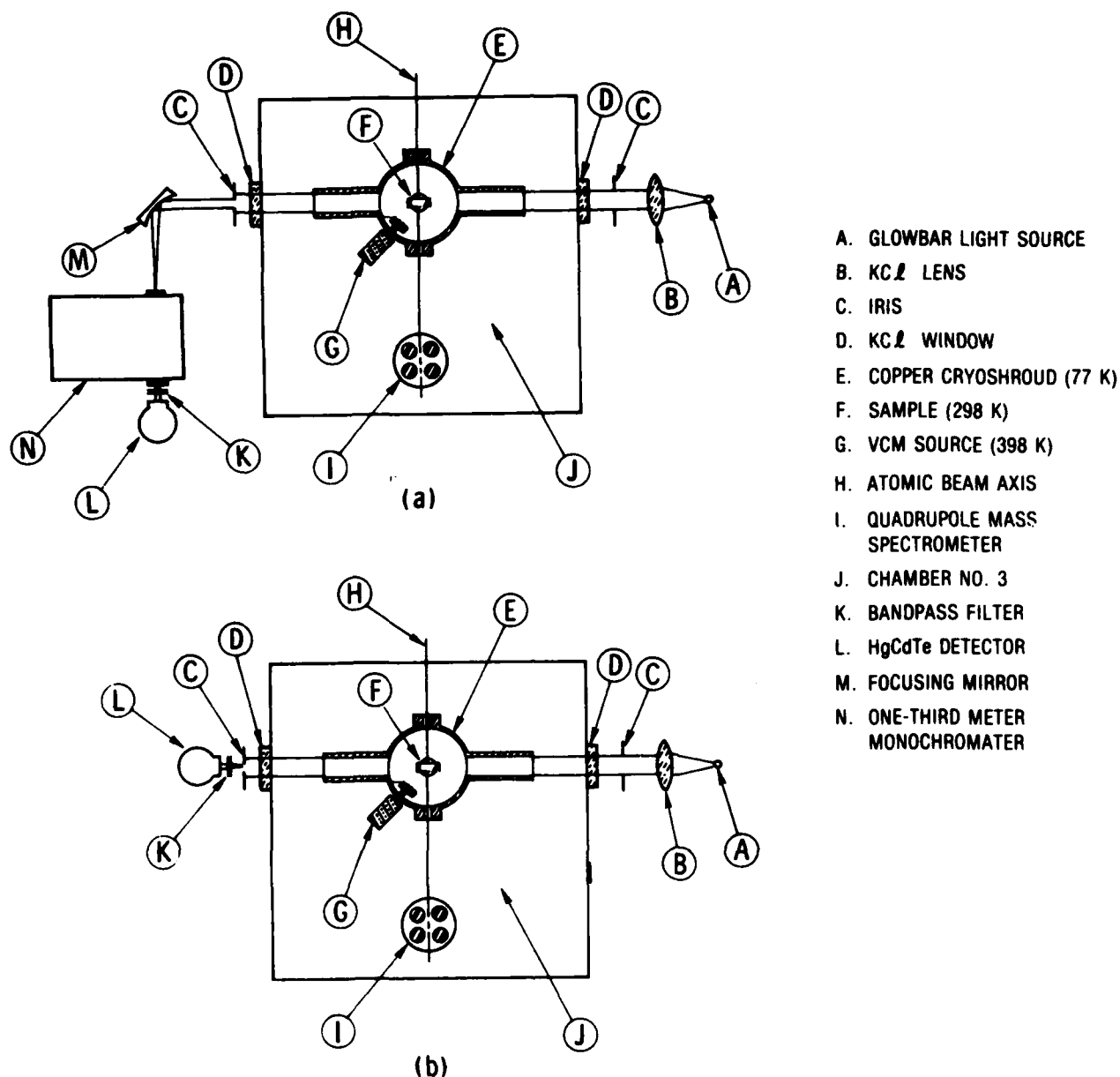M. FOCUSING MIRROR

N. ONE-THIRD METER MONOCHROMATER

Fig. 9. DMSP ESA Laboratory Experiment Optical System. (a) Spectral dispersion and (b) total transmission.

Volatile condensible materials (VCM), representative of satellite outgas-
sing impurities, could be deposited on the germanium flat by heating a sample
of the outgassing material, inside the cryoshroud. The VCM source was a brass
cylinder heated by six 10 W cartridge heaters (Hotwatt, Inc.) regulated by an
Omega Model 49 proportioning temperature control. The holder for the
outgassing material was inserted into the heated cylinder, secured by set
screws, and extended inside the cryoshroud. In all experiments reported here,
the outgassing material was GE RTV-615, polydimethylsiloxane, which had been
cured in air for 2 hr at 373 K. This contaminant was selected because
experimental data on a transmission spectra in the region of interest (in the
absence of oxygen atom bombardment) are available.[58] Furthermore because of
the heretofore mentioned inefficiency of oxygen plasma in removing silicon
containing surface contaminants, VCMs of this nature are considered to be a
likely source of difficulty.[31] During the deposition, the sample was raised
and rotated face-to-face with the VCM source. The exposed areas of the sample
and the outgassing material were of the same diameter, 19 mm, and were sepa-
rated by about 25 mm, thus approximately uniform coverage of the receiving
surface was provided. The typical outgassing period was 8 hr with the RTV
held at 373 K and the sample maintained at 298 K. After the deposition
period, the VCM source heaters were turned off and the source cooled rapidly
(by radiation to the cryoshroud).

V. RESULTS AND DISCUSSION

A. RESULTS

Seven separate experiments in which coated germanium flats were bombarded with an atomic beam were performed. The natures of these experiments are summarized in Table 6.

An initial experiment was performed to verify that the vacuum system was sufficiently clean. An OCLI long-pass coated germanium filter with a cut-on wavelength of 13.46 µm (L13460-9) was used. After it was mounted in the sample holder, the transmission spectrum of the sample was measured using a Perkin-Elmer 467 grating infrared spectrometer. The sample was then bombarded for 5-1/2 hr with an oxygen atom beam produced under the standard conditions described above. It was then removed from the system, in its holder, and its transmission spectrum measured again. The 467 spectrometer measured the transmission of the entire area of the disk while the atomic beam subtends only a small central portion. Any change in transmission across the entire area of the sample must result from spurious contamination from the vacuum system. No change in the transmission spectrum of the disk indicative of such contamination was observed.

The same sample was bombarded in the second experiment. This time the transmission spectrum of the sample was between 14 and 16 µm and was measured in situ before and after bombardment, with the light source and detector focused on the region of bombardment (see Fig. 9). Within the degree of uncertainty of the measurement, no effect was observed after 5-1/2 hr of bombardment. One must point out, however, that because of the long optical path of this experimental configuration, the signal-to-noise ratio of this measurement was poor. Thus the uncertainty in the measurement of the transmission spectrum was so great that an effect would need to have been dramatic to be observed.

The experimental procedure was altered to remedy this shortcoming. In order to increase the precision in the transmission measurement, we measured

Table 6. DMSP ESA Laboratory Experiment Conditions

Experiment No.	Sample	VCM Outgassing Conditions	Beam Source Conditions	Exposure Time (min)	Sample Analysis
1	OCLI L13460-9	N/A	19 Torr He: O_2 H_2O/90:10:1 100 W	326	Transmission spectrum measure 12.5 to 40 μm after exposure to air
2	OCLI L13460-9	N/A	19 Torr He: O_2 H_2O/90:10:1 100 W	330	Transmission spectrum measured 14 to 16 μm in situ
3	OCLI L13460-9	N/A	19 Torr He: O_2 H_2O/90:10:1 100 W	360	Transmission over 14 to 16 μm measured in situ
4	OCLI L13460-9	GE RTV 615:373 K Sample :298 K Exposure :500 min	19 Torr He: O_2 H_2O/90:10:1 100 W	540	As experiment No. 3
5	OCLI L08261-9	GE RTV 615:376 K Sample :298 K Exposure :430 min	19 Torr He: O_2 H_2O/90:10:1 100 W	492	As experiment No. 3 and transmission spectrum measured after exposure to air
6	OCLI L13460-9	GG RTV 615 :371 K Sample :298 K Exposure :450 min	20 Torr He 100 W	593	As experiment No. 3
7	OCLI 6040005-ST	GE RTV 615 :377 K Sample :290 K Exposure :480 min	7.7 Torr O_2 100 W	685	As experiment No. 5

54

the transmission of the sample across the entire 14 to 16 μm band before and after 6 hr of bombardment. The measured transmission of the OCLI 13460-9 disk was 79.4% before bombardment and 79.7% after bombardment. Since the uncertainty in this measurement is of the order of 3 percentage points, the difference between these two values is not significant.

In all three of the experiments described above, samples were bombarded under the standard beam conditions in the absence of any added surface contaminant. In the fourth experiment the sample was coated with a VCM before bombardment (Table 6). The sample used was a previously untreated OCLI 613460-9 filter; the VCM source was GE RTV-615. The transmission between 14 and 16 μm (measured as in experiment 3) was 69.9% before VCM deposition, 72.9% after VCM deposition, and 73.0% after 9 hr bombardment. Differences in these numbers are not considered significant. Inspection of the sample after its exposure to air revealed that because of misalignment of the apparatus during VCM deposition, only half of the sample surface was coated with the impurity.

This experiment was, accordingly, repeated. The sample bombarded was a clean OCLI-L08261-9 long pass filter with a cut-on wavelength of 8.26 μm. Transmission of the filter was measured with the Perkin-Elmer 467 spectrometer before installation in the apparatus. Transmission measured in situ over the 14 to 16 μm band was 51.6% before VCM deposition, 50.4% after VCM deposition, and 51.9% after 8.2 hr of bombardment. These differences are not considered significant. Although no effect on the 14 to 16 μm transmission was observed, there was a visible change in the VCM film over the area subtended by the atomic beam. The area subjected to bombardment by the beam appeared to be white, opaque to the eye, and rough, whereas unbombarded VCM films were smooth and transparent. Measurement of the transmission spectrum of the sample (after it was exposed to air) using the Perkin-Elmer 467 confirmed the absence of any effect in the 14 to 16 μm band and showed only absorptions attributable to the virgin VCM film.[58] Thus the visibly altered area was not different to the pure VCM in its transmission between 8.3 and 25 μm. The substrate itself was opaque at longer and shorter wavelengths, rendering further spectroscopic measurements impossible.

Because the source produces species other than oxygen atoms, the alteration to the VCM observed in experiment 5 cannot unambiguously be ascribed to the action of atomic oxygen. The source also produces, as we have noted above, light, and very probably metastable excited helium. In order to attempt to discern the effect of oxygen atoms from those of other products of the source, two other experiments were performed.

An OCLI 13460-9 filter was treated with RTV-615 VCM and subjected for 10 hr to bombardment by the products of a discharge of pure helium. The 14 to 16 μm transmission of the sample was 75.5% before deposition, 67.4% after deposition, and 74.5% after bombardment. The apparent reduction in transmission by the untreated VCM is difficult to explain inasmuch as it is at odds with other experiments reported here and elsewhere.[58] Although the 14 to 16 μm transmission of the sample was not different before treatment and after bombardment, there was again a visible change in the appearance of the VCM film. The area subtended by the beam source appeared darkened and opaque to the eye. Because the sample is opaque at wavelengths shorter than 13.46 μm, spectroscopic investigation of this visibly altered area was not possible.

In the final experiment, an OCLI-6040005ST filter was used. This filter was not selected to provide an outermost layer identical to that on the DMSP ESA objective lense. This multilayer antireflection-coated germanium filter is transparent to wavelengths longer than 1.8 μm, thus it permits more extensive spectroscopic analysis of experimental results. Transmission of the sample over the 14 to 16 μm band was 59.6% before VCM deposition, 58.5% after VCM deposition (not significantly different), and 77.6% after 11-1/2 hr bombardment by the beam produced by discharging 7.7 Torr of neat O_2. (A longer exposure time was used because the source operating on pure O_2 produces a lower absolute flux of oxygen atoms). The large change in transmission after oxygen atom bombardment was surprising, especially in light of the fact that the 14 to 16 μm transmission of the sample after VCM deposition and bombardment was greater than that for the clean sample. Inspection of the sample after its exposure to air showed a transparent coating over the entire area with a noticeable ring surrounding the area of bombardment (perhaps indicating

a difference in coating thickness in the area bombarded). Spectroscopic examination of the sample with the P-E 467 tended to confirm that the bombarded area was more transparent in the LWIR than the unbombarded area (Fig. 10). No sharp absorption features were observed other than those which could be ascribed to virgin VCM on either area.

B.   DISCUSSION

Experiments 1, 2, and 3 show that the LWIR transmission of these dielectric-coated germanium optics is not affected by bombardment by oxygen atoms at velocities less than 2.5 km sec^{-1}. This unambiguous result does not, however, necessarily imply that oxygen atoms impinging on these surfaces at orbital velocity will have no effect as well.

Experiments 4 through 7 imply that there is no dramatic effect on the LWIR transmission VCMs produced from polydimethylsiloxane. Bombarded samples showed no absorption features that differed from those of the untreated VCM. Experiment 7 did show some change in the LWIR transmission of the sample. However this alteration was manifest as an increase in the total transmission at all wavelengths longer than 5 μm, upon which the same siloxane VCM absorption bands appeared. No definite explanation of this result may be offered here, but it is reasonable to suggest that this difference is a result of a change in the thickness of the contaminant layer caused by bombardment. (The appearance at the sample certainly supports this suggestion.) Extra layers of different thickness will most probably alter the properties of already complex multilayer coatings in different ways. It is not possible to surmise from the data available how the impinging beam may have caused such an alteration. Possible mechanisms are ablation by oxygen atoms, ablation by excited O_2 in the beam, and photolysis.

Although there were no clearly discernible effects to the bombarded contaminant films in their LWIR transmission, effects resulting from the bombardment were apparent (see above). Further spectroscopic investigations of these affected surfaces were not possible because of the limited transmission range of the substrates and the already complex reflectance spectrum of the multilayer dielectric coatings of the germanium disks. The
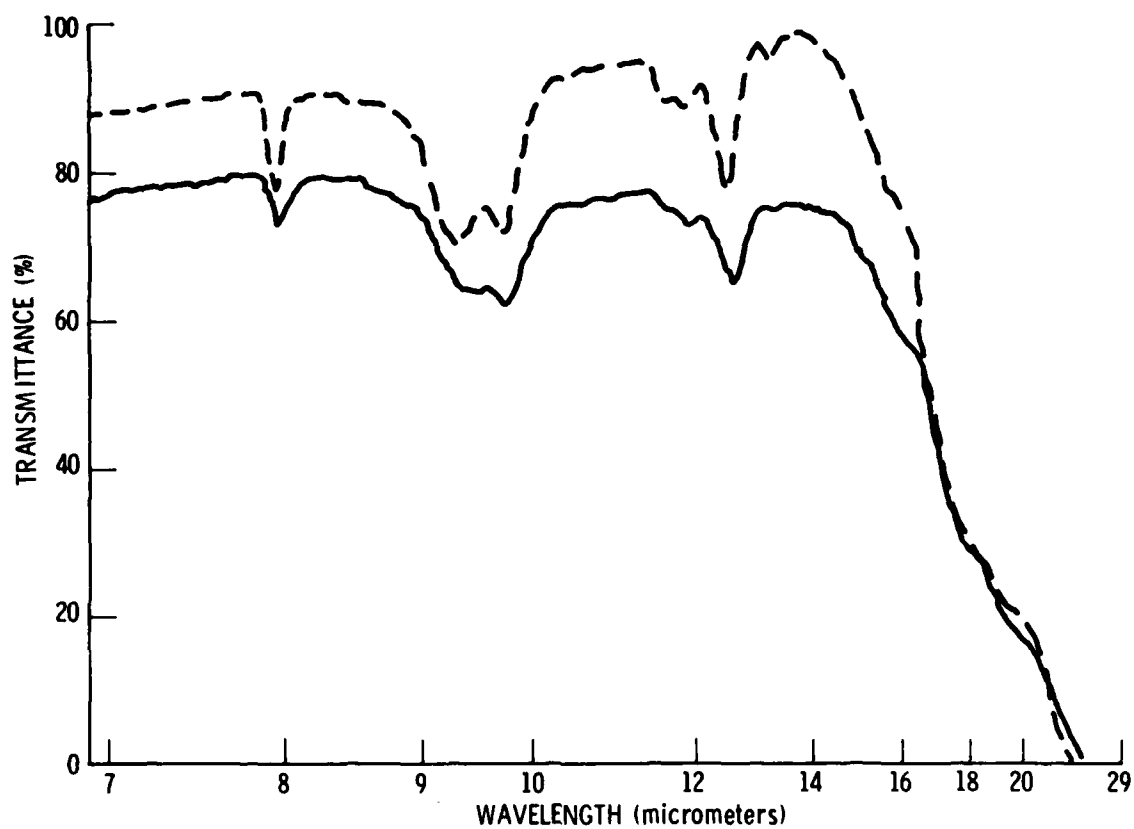
Fig. 10.   Transmission Spectra.   Results of experiment 7 (dashed line, bombarded area; solid line area not bombarded, refer to text.)

58

appearance of the three bombarded contaminant films (cf experiments 5, 6, and 7) was different, but it is not possible unambiguously to ascribe these differences to the variation in oxygen atom flux of the three bombarding beams. In at least one qualitative way, opacity to the eye, the severity of the effect on the film increased with increasing brightness of the beam source (Table 5).

That the results of this experimental program are in part ambiguous points out the difficulty inherent in performing such measurements. These experiments were required to elucidate the integrated effect of long exposure to the low orbit environment. In order to fulfill this role properly, an experiment first must isolate an agent of that environment, in this case, neutral oxygen atom bombardment. The experiment furthermore must simulate the orbital experience sufficiently closely to ensure that any effect observed (or not observed) can reasonably be expected to occur on orbit. Thus, a requirement of an integrated flux of 10^{23} m^{-2} of oxygen atoms impinging at 6 to 8 km sec^{-1} is imposed. Technological limitations forced us to accept the ambiguities introduced by using oxygen atoms of less than the desired velocity and by the flux of ultraviolet light emanating from the discharge source.

C. OUTLOOK FOR THE FUTURE

The experimental investigation of the effect of atmospheric bombardment of satellite surfaces by atomic oxygen is an ongoing effort in our laboratory. Facilities are currently under construction that will enable us to model more realistically the atmospheric oxygen atom flux. A DC arc atomic beam source, currently in its final stages of testing, has been built to produce an intense source of atomic oxygen at velocities up to 8 km/sec. The ultraviolet emission from this source will probably be more intense than that produced by the microwave discharge sources used heretofore. A slotted disk velocity selector[63] will be used to filter out this radiation to determine unambiguously the effects of oxygen atoms upon satellite surfaces. In addition, the molecular beam apparatus used in the DMSP ESA anomaly studies will be augmented by the addition of an ultrahigh vacuum chamber. Since this chamber will be pumped by a high speed turbomolecular pump, it will provide

the ultraclean environment necessary for the proper performance of beam-surface experiments. A schematic representation of the entire facility is shown in Fig. 11.

This facility will be used initially to measure the effect of high energy oxygen atom bombardment on the reflectivity of front surface mirrors and on the transmission of optical materials used in satellite sensors. These measurements will be done on both clean and contaminated (with satellite outgassed impurities) surfaces as a function of total oxygen atom flux and of incident velocity. These experiments will provide an important extension of the DMSP ESA study and will serve to resolve the ambiguities in the results presented above. This facility will also allow investigation of other surface phenomena which may be of importance in low orbit. Effects which could be addressed (and the programs, which indicate their potential importance) are sputtering (OGO-6), the volatilization of surface impurites (NIMBUS 6,7), and chemiluminescent surface reactions (AE-C).
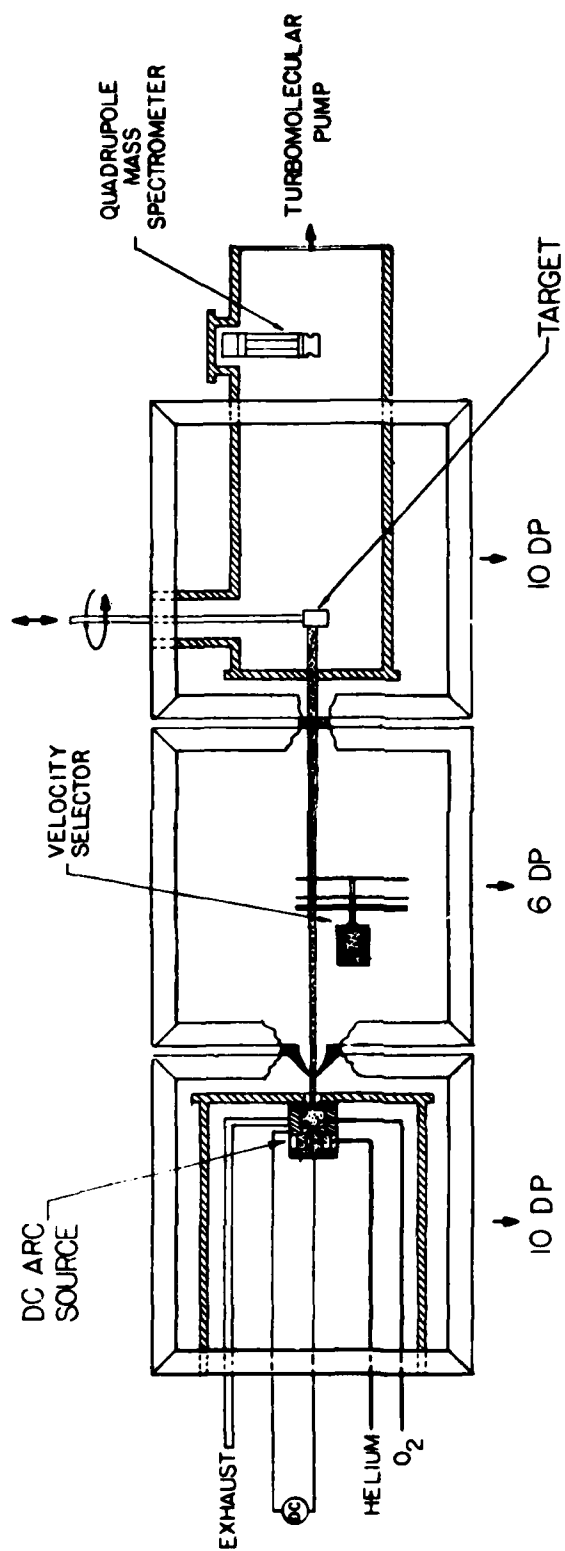
Fig. 11. High Energy Oxygen Atom Surface Chemistry Apparatus

REFERENCES

1. A. E. Hedin, "Tables of Thermospheric Temperature, Density and Composition Derived from Satellite and Ground Based Measurements," Vols. 1, 2, and 3, Laboratory of Planetary Atmospheres, GSFC, Greenbelt, Md. (January 1979).

2. A. E. Hedin, C. A. Reber, G. P. Newton, N. W. Spencer, H. C. Brinton, H. G. Mazer, and W. E. Pottes, "A Global Thermospheric Model Based on Mass Spectrometer and Incoherent Scatter Data MSIS 2 Composition," J. Geophysical Res. 82, 2148 (1977).

3. A. E. Hedin, J. E. Salah, J. V. Evans, C. A. Reber, G. P. Newton, H. W. Spencer, D. C. Kayer, D. Alcoydi, P. Bauer, L. Cogger and J. P. McClure, "A Global Thermospheric Model Based on Mass Spectrometer and Incoherent Scatter Data 1, N_2 Density and Temperature," J. Geophys. Res. 82, 2139 (1977).

4. F. S. Johnson, ed., Satellite Environment Handbook, Stanford University Press, Stanford, Calif. (1961) pp. 27-39.

5. M. R. Torr, P. B. Hays, B. C. Kennedy, and J. C. G. Walker, Planet. and Space Sci. 25, 173 (1977).

6. V. Abreu, University of Michigan, private communication.

7. D. McKeown, M. G. Fox, and J. J. Schmidt, "Measurement of Surface Erosion from Discoverer 26," ARS Journal 32, 954 (1962).

8. D. McKeown, M. G. Fox, J. J. Schmidt, and D. Hopper, "Sputtering in the Upper Atmosphere," AIAA Journal 2, 400 (1964).

9. D. McKeown, "Surface Erosion in Space," Proceedings of the Third International Symposium on Rarefied Gas Dynamics, Paris (1962), p. 315.

10. D. McKeown, "New Method for Measuring Spattering in the Region Near Threshold," Rev. Sci. Instrum. 32, 133 (1961).

11. D. McKeown and W. E. Corbin, Jr., "Space Measurements of the Contamination of Surfaces by OGO-6 Outgassing and Their Cleaning by Sputtering and Desorption," NBS Special Publication No. 336, Space Simulation, J. C. Richmond, ed. (October 1970), p. 113.

12. J. P. Simpson and F. C. Witteborn, Appl. Opt. 16, 2051 (1977).

13. N. M. Harvey and R. R. Herm, Helium Purge Flow Prevention of Atmospheric Contamination of the Cryogenically Cooled Optics of Orbiting Infrared Telescopes: Calculation of He-O Differential Cross Section, TR-0081(6432-03)-1, The Aerospace Corp., El Segundo Calif. (5 June 1981) (and references cited therein).

14. R. Predmore, "In-Orbit Degradation of Optics: TIROS/Block 5D ESA and NIMBUS ERB Sensors," NASA Goddard Memorandum (12 October 1969).

15. R. J. Madix and A. A. Sus, "Reactive Scattering of Atomic Oxygen From Clean Elemental Semiconductor Surfaces," Surf. Sci. 20, 277 (1970) (and references cited therein).

16. M. A. D. Fluendy and K. P. Lawley, Chemical Application of Molecular Beam Scattering, Chapman and Hall, London (1973), pp. 66-70.

17. G. N. K. Liu, "High Temperature Oxidation of Graphite by a Dissociated Oxygen Beam," MIT DSR 72803, AFOSR, Massachusetts Institute of Technology Aerophysics Laboratory, Cambridge, Mass. (August 1973) (Contract F44620-71-C-0009).

18. H. B. Niemann, "An Atomic Oxygen Beam System for the Investigation of Mass Spectrometer Response in the Upper Atmosphere," Rev. Sci. Instrum. 43, 1151 (1972).

19. A. E. Hedin, B. B. Hinton, G. A. Schmitt, "Role of Gas-Surface Interactions in the Reduction of Ogo 6 Neutral Particle Mass Spectrometer Data," J. Geophys. Res. 78, 4651 (1973).

20. G. W. Sjolander, "Atomic Oxygen-Metal Surface Studies as Applied to Mass Spectrometer Measurements of Upper Planetary Atmospheres," J. Geophys. Res. 81, 3767 (1976).

21. L. R. Lake and A. O. Nier, "Loss of Atomic Oxygen in Mass Spectrometer Ion Sources," J. Geophys. Res. 78, 1645 (1973).

22. D. Offermann and K. U. Grossmann, "Thermospheric Density and Composition as Determined by a Mass Spectrometer with Cryo Ion Source," J. Geophys. Res. 78, 8296 (1973).

23. H. B. Niemann and N. W. Spencer, "A Thermosphere Composition Measurement Using a Quadrupole Mass Spectometer with a Side Energy Focusing Quasi-Open Ion Source," J. Geophys. Res. 78, 2265 (1973).

24. L. R. Lake and K. Mauersberger, "Investigation of Atomic Oxygen in Mass Spectrometer Ion Sources," Int. J. Mass Spectrom. Ion Physics 13, 425 (1974).

25. J. L. Hayden, A. O. Nier, J. B. French, N. M. Reid, and R. J. Ducbett, "The Characteristics of an Open Source Mass Spectrometer Under Conditions Simulating Upper Atmosphere Flight," Int. J. Mass Spectrom. Ion Physics 15, 37 (1974).

26. B. J. Wood, "The Rate and Mechanism of Interaction of Oxygen Atoms and Hydrogen Atoms with Silver and Gold," J. Phys. Chem. 75, 2188 (1971).

27. B. J. Wood, B. R. Baker, and H. Wise, Research Related to Measurements of Atomic Species in Earth's Upper Atmosphere, Final Report Project PGU-6682, SRI (1970).

28. J. A. Riley and C. F. Giese, "Interaction of Atomic Oxygen with Various Surfaces," J. Chem. Phys. 53, 146 (1970).

29. G. S. Hollister, R. T. Brackman, and W. L. Fite, "The Use of Modulated Atomic Beam Techniques for the Study of Space-Flight Problems," Planet. Space Sci. 3 162 (1961).

30. R. B. Gillette and B. A. Kenyon, Appl. Opt., 10, 545 (1971).

31. R. B. Gillerre, J. R. Hollchem, and George L. Carlson, J. Vac. Sci. Tech, 7 534, 1970.

32. R. B. Gillette, W. D. Beverly, and G. A. Cruz, Active Cleaning Technique for Removing Contaminants from Optical Surfaces in Space, Annual Report No. 1. The Boeing Company, Seattle, Wash. (March 1972) (Contract NAS 8-26385).

33. R. B. Gillette, and W. D. Beverly, Paper No. 71-463 presented at AIAA 6th Thermophysics Conference, Tullahoma, Tenn. (April 1971).

34. R. L. Shannon and R. B. Gillette, Active Cleaning Technique Device, D180-18031-1, Boeing Aerospace Co., Seattle, Wash. (March 1973).

35. R. L. Shannon and R. B. Gillette, Laboratory Demonstration Model Active Cleaning Technique Device, D180-18031-1, Boeing Aerospace Co., Seattle, Wash. (March 1974).

36. W. J. Hays, W. E. Rogers, and E. L. Knuth, J. Chem Phys. 45 2175 (1972).

37. Shih-Min Liu, An Experimental Study of Interactions of Hyperthermal Atomic Beams with (11) Silver Surfaces and Absorbed Molecules, ENG-7510, School of Engineering and Applied Science, UCLA, Los Angeles, Calif. (February 1975).

38. (a) S. J. Sibener, R. J. Buss. C. Y. Ng, and Y. T. Lee, Rev. Sci. Instrum. 51, 167 (1980).
    (b) D. R. Miller and D. F. Patch, Rev. Sci. Instrum. 40, 1566 (1969).

39. R. H. Hansen, J. V. Pascale, T. De Benedictis, and P. N. Rentzepis, J. Polymer Sci. A, $\underline{3}$ 2205 (1965).

40. D. H. Reneker and L. H. Bulz, J. Macromol Sci-Chem $\underline{A10}$, 599 (1976).

41. M. A. D. Fluendy and K. P. Lawley, Op. Cit. pp. 65-87.

42. P. A. Gorry and R. Grice, "Microwave Discharge Source for the Production of Supersonic Atom and Free Radical Beams," J. Phys. E. $\underline{12}$, 857 (1979).

43. D. R. Peplinski, Crossed Beam Chemi-ionization Studies of Ba, Sr, Ca, La and Ce with Reactive Gases, M.S. Thesis, Ill. Inst. Tech. (1977).

44. W. S. Young, An Arc-Heated Ar-He Binary Supersonic Molecular Beam with Energies up to 21 eV, Report 69-39, School of Engineering and Applied Sciences, UCLA, Los Angeles, Calif. (July 1969).

45. R. W. Bickes et al., "Utilization of an Arc Heated Jet for the Production of Supersonic Seeded Beams of Atomic Nitrogen," J. Chem. Phys. $\underline{64}$, 3648 (1976).

46. K. R. Way, S. C. Young, and W. C. Stwalley, "A High Intensity Super-thermal Source of Hydrogen Atoms," ICPEAC IX. Abstracts of Papers, J. S. Risley and R. Geballe, eds., U. of Washington Press, Seattle, Wash. (1975).

47. K. R. Way, S. C. Young, and W. C. Stwalley, Rev. Sci. Instrum., $\underline{47}$, 1049 (1976).

48. E. L. Knuth, UCLA, private communication.

49. J. A. Silver, Aerodyne Research Co., private communication.

50. Systems Analysis Report Vol. 4: Attitude Determination and Control, Radio Corporation of Amerca, Princeton, N.J. (30 January 1976) (Contract FO4701-72-C-0221).

51. L. T. Greenberg, The Aerospace Corp., private communication.

52. K. Ward, The Relationship Between a Change in ESA Detector Offset and a Change in Measured Radiance, Barnes Project Report 2336, Barnes Engineering Co., Stamford Conn. (8 August 1979).

53. J. E. Sissala, ed., The Nimbus 6 User's Guide, Goddard Space Flight Center, NASA, (February 1975).

54. G. Nilsen, Optical Coating Lab., Inc., private communication.

55. J. Askill, Tracer Diffusion Data for Metals Alloys and Simple Oxides, IFI/Plenum, New York (1970).

56. K. J. Laidler, Chemical Kinetics, McGraw Hill, New York (1965), pp. 316-318.

57. G. A. Bird, "Spacecraft Outgas Ambient Flow Interaction," AIAA J. Spacecraft, 18, (1), 31 (1981).

58. R. W. Phillips, L. U. Tolentino, and S. Feuerstein, Spacecraft Contamination Under Simulated Orbital Environment, TR-0077(2270-30)-2, The Aerospace Corp., El Segundo, Calif. (6 July 1977).

59. E. J. Murphy and J. H. Brophy, Rev. Sci. Instrum. 50, 635 (1979).

60. F. C. Fehsenfeld, K. M. Evenson, and H. P. Broida, Rev. Sci. Instrum. 36, 294 (1965).

61. A. T. Zander, and G. M. Hieftje, Appl. Spec. 35, 357 (1981).

62. P. M. Houpt, and G. H. W. Baalhuis, Appl. Spec. 34, 89 (1980).

63. J. L. Kinsey, Rev. Sci. Instrum. 37, 61 (1966).

64. J. Hofman, "Mass Spectrometer Measurements of Ionosphere Composition" in Recent Developments in Mass Spectroscopy," Proceedings of the International Conference on Mass Spectroscopy, Kyoto, Japan (1969), pp. 1068-1072.

LABORATORY OPERATIONS

The Laboratory Operations of The Aerospace Corporation is conducting exper-
imental and theoretical investigations necessary for the evaluation and applica-
tion of scientific advances to new military space systems. Versatility and
flexibility have been developed to a high degree by the laboratory personnel in
dealing with the many problems encountered in the nation's rapidly developing
space systems. Expertise in the latest scientific developments is vital to the
accomplishment of tasks related to these problems. The laboratories that con-
tribute to this research are:

Aerophysics Laboratory: Launch vehicle and reentry aerodynamics and heat
transfer, propulsion chemistry and fluid mechanics, structural mechanics, flight
dynamics; high-temperature thermomechanics, gas kinetics and radiation; research
in environmental chemistry and contamination; cw and pulsed chemical laser
development including chemical kinetics, spectroscopy, optical resonators and
beam pointing, atmospheric propagation, laser effects and countermeasures.

Chemistry and Physics Laboratory: Atmospheric chemical reactions, atmo-
spheric optics, light scattering, state-specific chemical reactions and radia-
tion transport in rocket plumes, applied laser spectroscopy, laser chemistry,
battery electrochemistry, space vacuum and radiation effects on materials, lu-
brication and surface phenomena, thermionic emission, photosensitive materials
and detectors, atomic frequency standards, and bioenvironmental research and
monitoring.

Electronics Research Laboratory: Microelectronics, GaAs low-noise and
power devices, semiconductor lasers, electromagnetic and optical propagation
phenomena, quantum electronics, laser communications, lidar, and electro-optics;
communication sciences, applied electronics, semiconductor crystal and device
physics, radiometric imaging; millimeter-wave and microwave technology.

Information Sciences Research Office: Program verification, program trans-
lation, performance-sensitive system design, distributed architectures for
spaceborne computers, fault-tolerant computer systems, artificial intelligence,
and microelectronics applications.

Materials Sciences Laboratory: Development of new materials: metal matrix
composites, polymers, and new forms of carbon; component failure analysis and
reliability; fracture mechanics and stress corrosion; evaluation of materials in
space environment; materials performance in space transportation systems; anal-
ysis of systems vulnerability and survivability in enemy-induced environments.

Space Sciences Laboratory: Atmospheric and ionospheric physics, radiation
from the atmosphere, density and composition of the upper atmosphere, aurorae
and airglow; magnetospheric physics, cosmic rays, generation and propagation of
plasma waves in the magnetosphere; solar physics, infrared astronomy; the
effects of nuclear explosions, magnetic storms, and solar activity on the
earth's atmosphere, ionosphere, and magnetosphere; the effects of optical,
electromagnetic, and particulate radiations in space on space systems.